

**BIOMASS DERIVED CALCIUM OXIDE CATALYST FOR
BIODIESEL PRODUCTION FROM WASTE COOKING OIL**

SI SO JIE TING

**A project report submitted in partial fulfilment of the
requirements for the award of Bachelor of Engineering
(Honours) Chemical Engineering**

**Lee Kong Chian Faculty of Engineering and Science
Universiti Tunku Abdul Rahman**

May 2021

DECLARATION

I hereby declare that this project report is based on my original work except for citations and quotations which have been duly acknowledged. I also declare that it has not been previously and concurrently submitted for any other degree or award at UTAR or other institutions.

Signature :  _____

Name : SI SO JIE TING _____

ID No. : 1602331 _____

Date : 7 May 2021 _____

APPROVAL FOR SUBMISSION

I certify that this project report entitled “**BIOMASS DERIVED CALCIUM OXIDE CATALYST FOR BIODIESEL PRODUCTION FROM WASTE COOKING OIL**” was prepared by **SI SO JIE TING** has met the required standard for submission in partial fulfilment of the requirements for the award of Bachelor of Engineering (Honours) Chemical Engineering at Universiti Tunku Abdul Rahman.

Approved by,

Signature

:



Supervisor

:

Dr. Pang Yean Ling

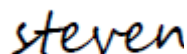
Date

:

7 May 2021

Signature

:



Co-Supervisor

:

Dr. Steven Lim

Date

:

7 May 2021

The copyright of this report belongs to the author under the terms of the copyright Act 1987 as qualified by Intellectual Property Policy of Universiti Tunku Abdul Rahman. Due acknowledgement shall always be made of the use of any material contained in, or derived from, this report.

© 2021, Si So Jie Ting. All right reserved.

ACKNOWLEDGEMENTS

I would like to take this opportunity to express my sincerest gratitude to everyone who had provided assistance for me to complete this research. First of all, I would like to convey my utmost gratitude to my supervisor, Dr. Pang Yean Ling for her invaluable guidance, advice and supervision throughout the development of this research.

Next, I would like to thank my loving family and friends who had given me useful suggestions, opinions, encouragement and constant mental support during my studies. Lastly, I would like to express my deepest thanks to all the researchers for their contributions in this field of study as I have gained a lot of valuable knowledge through their findings.

ABSTARCT

Recently, the discovery of biomass-derived calcium oxide (CaO) catalysts has made a remarkable improvement in the biodiesel industry in order to achieve the goal of green production. It was found that CaO catalysts could be prepared from a wide range of biomass sources. In the present study, the applications of several biomass-derived calcium oxide catalysts on the biodiesel production from waste cooking oil were evaluated based on the analysis from multiple journals. Furthermore, the characterisation results of the catalysts that obtained through several characterisation techniques were discussed and analysed in this study. The results from the characterisation studies revealed that the calcium carbonate (CaCO_3) in the biomass sources was decomposed into CaO by the calcination process. Next, Design Expert simulation was applied to examine the interaction effect between the parameters such as methanol to oil ratio, reaction duration, catalyst loading and temperature of reaction on biodiesel yield. The results revealed that the interaction between process parameters within the optimum operating ranges possessed a positive impact on the biodiesel yield. Then, the optimum operating conditions for different biomass-derived CaO catalyst models were then obtained through the application of response surface methodology (RSM). The present study proved that a variety of waste biomass can be utilised as a source of CaCO_3 to generate CaO catalyst through the calcination process, which can then be applied in the transesterification of waste cooking oil to produce a high yield of biodiesel. Furthermore, some recommendations for future research were also presented.

TABLE OF CONTENTS

DECLARATION		i
APPROVAL FOR SUBMISSION		ii
ACKNOWLEDGEMENTS		iv
ABSTARCT		v
TABLE OF CONTENTS		vi
LIST OF TABLES		viii
LIST OF FIGURES		x
LIST OF SYMBOLS / ABBREVIATIONS		xii
 CHAPTER		
1	INTRODUCTION	1
	1.1 Biodiesel as a Renewable Energy Source	1
	1.1.1 Advantages of Biodiesel	1
	1.1.2 Disadvantages of Biodiesel	2
	1.2 Feedstocks for Biodiesel Production	2
	1.3 Biodiesel Production	5
	1.3.1 Transesterification / Esterification	5
	1.3.2 Type of Catalyst Used	6
	1.4 Problem Statement	7
	1.5 Aim and Objectives	8
	1.6 Scope and Limitation of the Study	9
2	LITERATURE REVIEW	10
	2.1 Heterogeneous Catalysts	10
	2.1.1 Basic Catalyst	10
	2.1.2 Acid Catalyst	11
	2.2 Biomass Derived Catalyst	13
	2.2.1 Carbonisation of Biomass	15
	2.2.2 Biomass Derived Calcium Oxide Catalyst	19
	2.3 Mechanism for Biodiesel Production	20
	2.3.1 Acid Catalysed Transesterification	20
	2.3.2 Base Catalysed Transesterification	21

2.3.3	Calcium Oxide Catalysed Transesterification	21
2.4	Operating Parameters that Affect Biodiesel Production	23
2.5	Response Surface Methodology	25
2.5.1	Design Strategy for RSM	26
2.5.2	Model Fitting and Analysis	27
2.5.3	Optimisation	28
3	METHODOLOGY AND WORK PLAN	29
3.1	Documentary Analysis	29
3.1.1	Searching for Related Published Works	29
3.1.2	Study Selection and Data Collection	29
3.2	Catalyst Characterisation Studies	30
3.3	Response Surface Methodology for Calcium Oxide Catalysed Transesterification	31
4	RESULTS AND DISCUSSION	35
4.1	Analysis of Catalyst Characterisation Studies	35
4.1.1	Scanning Electron Microscopy with Energy X-ray Spectroscopy (SEM-EDX) Analysis	35
4.1.2	Brunauer-Emmett-Teller (BET) Surface Area Analysis	37
4.1.3	Thermogravimetric Analysis (TGA)	37
4.1.4	Fourier Transform Infrared Spectroscopy (FTIR)	40
4.1.5	X-ray Diffraction (XRD) Analysis	45
4.2	Design Expert Simulation	47
4.2.1	Development of Regression Model and Model Accuracy Check	47
4.2.2	Interaction between Parameters	63
4.2.3	Optimisation of Process Parameters	74
5	CONCLUSIONS AND RECOMMENDATIONS	77
5.1	Conclusions	77
5.2	Recommendations for Future Work	78
	REFERENCES	80

LIST OF TABLES

Table 1.1:	Classification of Feedstocks Used in Biodiesel Production (Abdullah, et al., 2017).	3
Table 1.2:	Estimated Amount of Waste Cooking Oil Generated in Specific Countries (Gui, Lee and Bhatia, 2008).	4
Table 2.1:	Biomass-Derived Solid Catalysts Used in Biodiesel Production.	14
Table 3.1:	Range and Levels of the Process Parameters for Optimisation of Biodiesel Production Process that Involved Chicken Eggshell-Derived CaO Catalyst (Tan, et al., 2017).	32
Table 3.2:	Range and Levels of the Process Parameters for Optimisation of Biodiesel Production Process that Involved Ostrich Eggshell-Derived CaO Catalyst (Tan, et al., 2017).	32
Table 3.3:	Range and Levels of the Process Parameters for Optimisation of Biodiesel Production Process that Involved Snail Shell-Derived CaO Catalyst (Gendy, Deriase and Hamdy, 2014).	33
Table 3.4:	Range and Levels of the Process Parameters for Optimisation of Biodiesel Production Process that Involved <i>Donax deltoides</i> Shell-Derived CaO Catalyst (Niju, Vishnupriya and Balajji, 2019).	33
Table 3.5:	Range and Levels of the Process Parameters for Optimisation of Biodiesel Production Process that Involved <i>Malleus malleus</i> Shell-Derived CaO Catalyst (Rabia, et al., 2018).	33
Table 4.1:	BET Surface Area and Pore Volume of Various Biomass-Derived CaO Catalysts.	38
Table 4.2:	TGA Analysis of Various Biomass-Derived CaO Catalysts.	40
Table 4.3:	FTIR Analysis of Various Biomass-Derived CaO Catalysts.	43
Table 4.4:	XRD Analysis of Various Biomass-Derived CaO Catalysts.	46
Table 4.5:	Experiment Matrix and Response for CaO Catalyst Derived from Chicken Eggshell.	48
Table 4.6:	Experiment Matrix and Response for CaO Catalyst Derived from Ostrich Eggshell.	50
Table 4.7:	Experiment Matrix and Response for CaO Catalyst Derived from Snail Shell.	52

Table 4.8:	Experiment Matrix and Response for CaO Catalyst Derived from <i>Donax deltoides</i> Shell.	53
Table 4.9:	Experiment Matrix and Response for CaO Catalyst Derived from <i>Malleus malleus</i> Shell.	54
Table 4.10:	ANOVA and Fit Statistics Results for Chicken Eggshell-Derived CaO Catalyst Model.	55
Table 4.11:	ANOVA and Fit Statistics Results for Ostrich Eggshell-Derived CaO Catalyst Model.	56
Table 4.12:	ANOVA and Fit Statistics Results for Snail Shell-Derived CaO Catalyst Model.	57
Table 4.13:	ANOVA and Fit Statistics Results for <i>Donax deltoides</i> Shell-Derived CaO Catalyst Model.	58
Table 4.14:	ANOVA and Fit Statistics Results for <i>Malleus malleus</i> Shell-Derived CaO Catalyst Model.	59
Table 4.15:	Constraints Used to Optimise the Biodiesel Yield.	75
Table 4.16:	Optimum Operating Conditions for Biodiesel Production for Each Model.	76

LIST OF FIGURES

Figure 1.1: Transesterification Process (Borges and Díaz, 2012).	5
Figure 1.2: Esterification Process (Borges and Díaz, 2012).	6
Figure 2.1: Effect of Carbonisation Time and Carbonisation Temperature on Ester Yield (Liu, et al., 2013).	17
Figure 2.2: Effect of Carbonisation Time on FAME Yield and Total Acid Density of Prepared Catalyst (Wong, et al., 2020).	18
Figure 2.3: Effect of Carbonisation Temperature on FAME Yield and Total Acid Density of Prepared Catalyst (Wong, et al., 2020).	18
Figure 2.4: Mechanism of Acid Catalysed Transesterification (Deshpande, Sunol and Philippidis, 2017).	20
Figure 2.5: Mechanism of Base Catalysed Transesterification (Meher, Vidyasagar and Naik, 2016).	21
Figure 2.6: Mechanism of CaO Catalysed Transesterification (Bharti, et al., 2020).	22
Figure 4.1: SEM Images of (a) Uncalcined Chicken Eggshell (Bharti, et al., 2020), (b) Uncalcined Ostrich Eggshell (Tan, et al., 2015), (c) Calcined Chicken Eggshell (Bharti, et al., 2020), (d) Calcined Ostrich Eggshell (Tan, et al., 2015), (e) Calcined <i>Donax deltoidea</i> Shell (Niju, Vishnupriya and Balajii, 2019) and (f) Calcined <i>Malleus malleus</i> Shell (Rabia, et al., 2018).	36
Figure 4.2: TGA Analysis of Chicken Eggshells (Fayyazi, et al., 2018).	39
Figure 4.3: FTIR Spectra of (a) Chicken Eggshells Samples (Bharti, et al., 2020), (b) <i>Donax deltoidea</i> Shells Samples (Niju, Vishnupriya and Balajii, 2019), (c) Ostrich Eggshells Samples (Tan, et al., 2015), (d) Snail Shells Samples (Gendy, Deriase and Hamdy, 2014), (e) <i>Pomacea</i> sp. Shells Samples (Margaretha, et al., 2012) and (f) Bottom Ashes Samples (Maneerung, Kawi and Wang, 2015).	42

- Figure 4.4: XRD Patterns of (a) Commercial CaO, Calcined Commercial CaO (Pure CaO), Calcined Chicken Eggshell and Calcined Ostrich Eggshell (Tan, et al., 2015), (b) Calcined *Donax deltoides* Shell (Niju, Vishnupriya and Balajii, 2019), (c) Calcined *Malleus malleus* Shell (Rabia, et al., 2018), (d) Calcined *Pomacea* sp. Shell (Margaretha, et al., 2012), (e) Calcined Bottom Ash (Maneerung, Kawi and Wang, 2015) and (f) Calcined Snail Shell (Gendy, Deriase and Hamdy, 2014). 47
- Figure 4.5: Normal Plot of Residuals for the (a) Chicken Eggshell Model, (b) Ostrich Eggshell Model, (c) Snail Shell Model, (d) *Donax deltoides* Shell Model and (e) *Malleus malleus* Shell Model. 62
- Figure 4.6: Interaction Effect between Methanol to Oil Ratio and Catalyst Concentration on Biodiesel Yield for the (a) Ostrich Eggshell Model, (b) Snail Shell Model and (c) *Donax deltoides* Shell Model. 64
- Figure 4.7: Interaction Effect between Methanol to Oil Ratio and Reaction Time on Biodiesel Yield for the (a) Snail Shell Model and (b) *Donax deltoides* Shell Model. 66
- Figure 4.8: Interaction Effect between Catalyst Concentration and Reaction Time on Biodiesel Yield for the (a) Chicken Eggshell Model, (b) Ostrich Eggshell Model and (c) *Malleus malleus* Shell Model. 68
- Figure 4.9: Interaction Effect between Methanol to Oil Ratio and Reaction Temperature on Biodiesel Yield for the Chicken Eggshell Model. 69
- Figure 4.10: Interaction Effect between Catalyst Concentration and Reaction Temperature on Biodiesel Yield for the (a) Chicken Eggshell Model and (b) Ostrich Eggshell Model. 71
- Figure 4.11: Interaction Effect between Reaction Time and Reaction Temperature on Biodiesel Yield for the (a) Chicken Eggshell Model and (b) Ostrich Eggshell Model. 73

LIST OF SYMBOLS / ABBREVIATIONS

<i>C</i>	conversion, %
<i>Y</i>	yield, %
ANOVA	analysis of variance
BET	Brunauer-Emmett-Teller
BBD	Box-Behnken design
CCD	central composite design
CaO	calcium oxide
CaCO ₃	calcium carbonate
Ca(OH) ₂	calcium hydroxide
CO ₃ ²⁻	carbonate molecule
<i>R</i> ²	coefficient of determination
DD	Doehlert design
FFD	full factorial design
FAME	fatty acid methyl esters
FFA	free fatty acids
FTIR	Fourier Transform Infrared spectroscopy
RSM	response surface methodology
SEM-EDX	Scanning Electron Microscopy with Energy Dispersive X-ray spectroscopy
TGA	Thermogravimetric analysis
XRD	X-ray diffraction

CHAPTER 1

INTRODUCTION

1.1 Biodiesel as a Renewable Energy Source

Fast development and rapid growth of population all around the world accelerate the consumption of energy sources. Fossil fuels, which are categorised as non-renewable sources, are widely employed in the transportation industry to power the combustion engines. However, fossil fuels replenish at a very slow rate as it takes millions of years to form. In view of the global demands, it is predicted that fossil fuels will deplete in the next 10 decades if no new sources are found (Lam, Lee and Mohamed, 2010). The depletion of fossil fuels associated with the environmental issues emerging from the burning of fossil fuels has called for a need to look for alternative sources in order to replace fossil fuels.

Among all alternative sources that have been investigated, biodiesel has grabbed the world's attention due to its superior properties to be an alternative for the conventional fuel used in diesel engines. Biodiesel is considered a type of sustainable energy source because it is renewable, biodegradable and more environmentally friendly compared to the petroleum diesel. The other term for biodiesel is fatty acid methyl esters (FAME). Biodiesel exhibits similar properties as diesel fuel. Therefore, no modification has to be done in the engine part when biodiesel is applied in engines (Mishra, 2012).

1.1.1 Advantages of Biodiesel

One of the well-known advantages of biodiesel is it has a wide variety of feedstocks. It can be derived from palm oil, animal fats, vegetable oils, waste oils, soybeans, corn or other crops that are easily available elsewhere. As compared to conventional diesel fuel, carbon dioxide emissions can be reduced by 78 % during the combustion of biodiesel (Takeuchi, et al., 2018). Biodiesel also produces less carbon monoxide, polycyclic aromatic hydrocarbons and sulphur. This can then help to cope with the problem of global warming and acid rain.

Moreover, biodiesel has higher combustion efficiency as it is an oxygenated fuel. The existence of oxygen in biodiesel aids in the combustion process (Verma, et al., 2019). Next, the production of biodiesel is not as complex as petroleum diesel since it does not involve processes such as drilling and refining. In addition, biodiesel is safer for handling, storage and transportation because it has a high flash point that exceeds 130 °C. This is considerably higher compared to the flash point of petroleum diesel which is 52 °C. Not only that, it is also found that biodiesel has great lubricating properties which can extend engine life and enhance engine efficiency by reducing wear and tear (Mishra, 2012). Biodiesel is miscible with petroleum diesel and they can be blended at different ratios to compensate for the environmental impacts caused by petroleum diesel.

1.1.2 Disadvantages of Biodiesel

Biodiesel has lower volatility and higher viscosity than conventional diesel fuel. These properties lead to carbon deposition in the engine part due to incomplete combustion (Agarwal, Bijwe and Das, 2003). However, this only occurs after a long operating time. It may also experience pumping difficulty due to its higher viscosity. Next, the high demand for biodiesel may create a food crisis since some of its feedstocks are comprised of food crops such as corn, maize, soybeans and vegetable oils. There are also some environmental pollution issues arising from the production of biodiesel which are the generation of waste and soap formation during the transesterification process.

Furthermore, the emission of nitrogen oxides in the combustion of biodiesel is higher than that of petroleum diesel. Besides that, biodiesel is less oxidative stable and it can be oxidised easily in the presence of air to form fatty acids (Zuleta, et al., 2012). This will lead to corrosion and coking in fuel injectors. In addition, biodiesel is not suitable to be used in the winter season because it will crystallise at a low temperature and cause cold start problems.

1.2 Feedstocks for Biodiesel Production

Biodiesel can be synthesised from different types of feedstocks. It can be categorised into first-generation biodiesel, second-generation biodiesel and third-generation biodiesel based on the types of feedstock used. Table 1.1

shows the classification of feedstocks utilised in the biodiesel production. First-generation biodiesel is generated from edible oils. For instance, it is produced from food crops like corn oil, coconut oil, peanut oil, soybean oil and palm oil. However, feedstocks for first-generation biodiesel become unsustainable as foods are used for fuel production. This has created awareness regarding food security and may lead to problems such as food shortage. Due to the increasing demand for biodiesel, second-generation biodiesel becomes more popular and is suggested to replace first-generation biodiesel as it has no impact on food issues. The feedstocks for second-generation biodiesel are comprised of non-edible oils, animal fats and waste oils. Next, algae are also considered as one of the feedstocks used in the production of biodiesel. It is enriched in lipid and can be grown largely within a short period of time (Khan, et al., 2017). Biodiesel generated from algae is known as third-generation biodiesel.

Table 1.1: Classification of Feedstocks Used in Biodiesel Production
(Abdullah, et al., 2017).

Biodiesel	Biodiesel Feedstocks	Examples
First-generation biodiesel	Edible oils	Wheat, Palm, Corn, Peanut, Coconut, Canola, Rapeseed
Second-generation biodiesel	Non-edible oils	Jatropha curcas, Tobacco seed, Rubber seed
	Waste or recycled oils	Waste cooking oil
	Animal fats	Chicken fats, Beef tallow, Fish oil
Third-generation biodiesel	Algae	Chlorophyceae

In fact, the cost of the feedstock is a significant variable affecting the total production cost of biodiesel. About 88 % of the cost for biodiesel production was contributed by the cost of feedstock (Lam, Lee and Mohamed, 2010). Hence, the selection of biodiesel's feedstock is quite important as the

main focus for the production of biodiesel is its economic viability. Among all existing feedstocks, waste oil or waste cooking oil is the best choice as it is low cost and easily available. The amount of waste cooking oil produced in each day is extremely large. Around 2 million tonnes of waste cooking oil are produced in America daily (Lam, Lee and Mohamed, 2010). In large countries such as China, about 10000 tonnes of waste cooking oil were produced daily (Gui, Lee and Bhatia, 2008). The estimated amount of waste cooking oil produced by some countries is shown in Table 1.2. These huge quantities of waste cooking oil generated may result in environmental pollution or contamination if no proper treatment is carried out.

Table 1.2: Estimated Amount of Waste Cooking Oil Generated in Specific Countries (Gui, Lee and Bhatia, 2008).

Country	Quantity (million tonnes/year)
Canada	0.12
China	4.5
European	0.7 - 1.0
Japan	0.45 - 0.57
Malaysia	0.5
United States	10.0

From Table 1.2, the amount of waste cooking oil generated by those countries has exceeds 16 million tonnes in a year. There are so many restaurants, food stalls and households all around the world where the exact quantity of waste cooking oil produced is immeasurable. The actual amount is much higher than this value based on the global scale. Therefore, it is sufficient to meet the global demand for biodiesel if waste oil or used oil is utilised as the feedstock. Moreover, a recent study shows that the overall cost of biodiesel production reduced by 60 % when waste cooking oil is used as compared to vegetable oil (Sarno and Iuliano, 2019). The utilisation of waste cooking oil in the production of biodiesel can reduce the waste oil disposal problems. The availability of waste cooking oil and low cost of production has made it become a favourable choice as feedstock in biodiesel production.

1.3 Biodiesel Production

Biodiesel or FAME can be produced through different methods. In general, most of the biodiesels are produced through the reactions of esterification and transesterification with the aid of catalyst as both reactions provide better conversion efficiency.

1.3.1 Transesterification / Esterification

Transesterification is a reversible process where one mole of triglyceride from the vegetable oils or animal fats reacts with three moles of alcohol to generate three moles of FAME and one mole of glycerol (Borges and Díaz, 2012). Glycerol is the by-product of this reaction. Ethanol and methanol are the common alcohol employed in the transesterification reaction. However, methanol is preferred as it is cheaper and easier to recover. Sometimes, co-solvent such as diethyl ether is added to improve the miscibility between oil and alcohol (Bharti, et al., 2020). Transesterification consists of three stepwise reactions. The complete transesterification process is shown in Figure 1.1. The triglyceride is first transformed to diglycerides. Then, the diglycerides converted to monoglyceride and finally into glycerol.

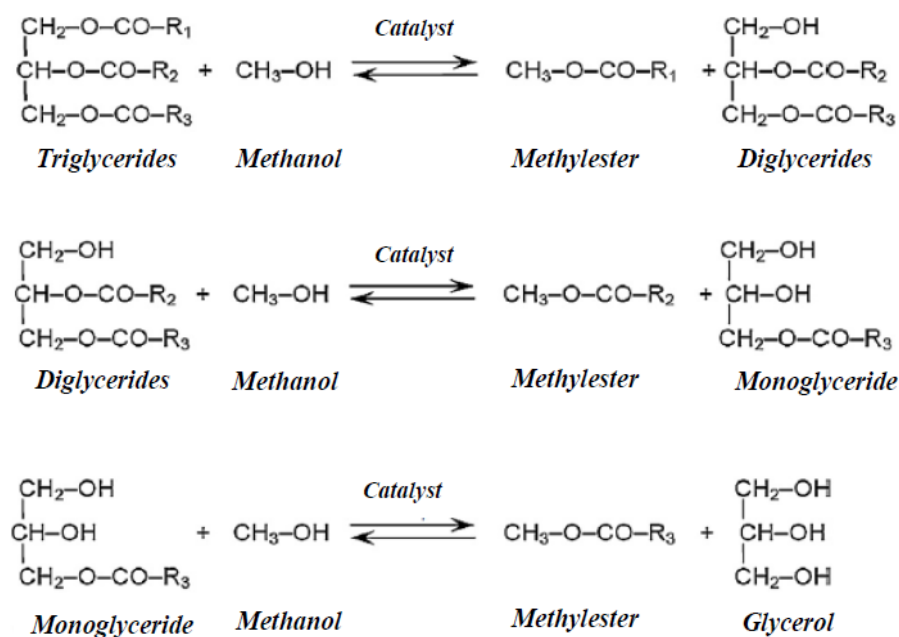


Figure 1.1: Transesterification Process (Borges and Díaz, 2012).

Transesterification of fats or oils with high free fatty acids (FFA) content will lead to soap formation and results in the reduction of biodiesel yield (Bharti, et al., 2020). In this case, the esterification process provides a more appropriate way for the synthesis of biodiesel as it can convert FFA effectively. The reaction for the esterification process is shown in Figure 1.2. During esterification, oils with high FFA content can be treated with alcohol to produce FAME and water. Different from transesterification, esterification reaction is only a one-step process.

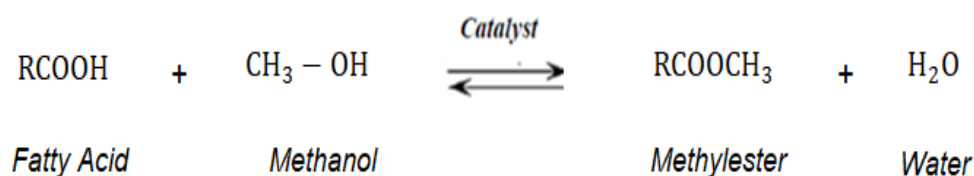


Figure 1.2: Esterification Process (Borges and Díaz, 2012).

1.3.2 Type of Catalyst Used

The use of catalyst is important in the production of biodiesel. Catalyst is used in the esterification and transesterification process to promote the reaction rate and increase the FAME yield. The catalyst used can be categorised into three major categories which are homogeneous catalysts, heterogeneous catalysts and enzyme catalysts. Next, it can be further classified into acid catalysts and alkaline or basic catalysts. Homogeneous catalysts and heterogeneous catalysts are commonly used in industry as they can be easily obtained.

Generally, acid catalyst is used in the esterification process as it is capable to convert those high FFA feedstocks into biodiesel (Sarno and Iuliano, 2019). Concentrated sulphuric acid is the most widely used acid catalyst in the esterification process and it is also an example of a homogeneous catalyst. For the transesterification reaction, it can be catalysed by acid catalyst and alkaline catalyst. The most popular catalyst used in this reaction is sodium hydroxide, which is an alkaline catalyst.

1.4 Problem Statement

Edible oils have been widely utilised as feedstocks for the production of biodiesel. However, the application of edible oils as biodiesel's feedstock is impractical for long-term production and it gives rise to many problems such as the rise in food prices, food versus fuel issues and deforestation. In order to fulfil the global demand for biodiesel, large areas of land are currently used to grow crops for biodiesel production instead of human consumption. More and more people have voiced out their dissatisfaction toward this practice, arguing that biodiesel production using edible oils is competing for food resources with the communities.

Moreover, Domingues, et al. (2012) reported that the production cost of biodiesel was about 2.5 times higher than the production cost of petroleum diesel. This is a major drawback for biodiesel to compete with conventional petroleum diesel. It was also found that the cost of feedstock largely contributed to the overall cost of production for biodiesel. Hence, the selection of a cheaper feedstock becomes crucial for biodiesel production to minimize the overall production cost and make it more competitive in the global market. Various alternative feedstocks have been proposed to address this concern. Non-edible oil appears to be a great alternative to replace edible oil as it is cheap and easily available. Furthermore, the application of waste cooking oil as the feedstock can help to solve the problem concerning the food versus fuel issue.

Next, the search for an appropriate catalyst is essential to achieve a sustainable production of biodiesel. The catalyst used must be low cost, environmentally friendly and exhibits good catalytic ability. However, most of the conventional catalysts do not meet these requirements. The discovery of biomass-derived catalysts has made a remarkable improvement in the biodiesel industry in order to achieve the goal of green production. Large quantities of waste including biomass waste are produced every day throughout the world but most of the wastes generated usually end up in landfills without proper treatment (Ferronato and Torretta, 2019). The application of biomass to synthesise catalysts can reduce landfill waste as well as promote a more environmentally friendlier and sustainable production of biodiesel. Furthermore, it is cheaper to synthesise the catalyst using biomass as

compared to the cost of conventional catalysts. It is notable that not all biomass can be used to synthesise the catalyst. Study and research should be carried out in order to find an effective and suitable biomass-derived catalyst for the sustainable production of biodiesel.

1.5 Aim and Objectives

The overall purpose of this research project is to reveal the potential of using biomass-derived catalyst for biodiesel production where waste cooking oil is used as feedstock. Generally, this research project is aimed to accomplish the following objectives:

- To review the characterisation studies of calcium oxide (CaO) catalyst synthesised from different biomass for biodiesel production.
- To investigate the interaction effect between process parameters and compare the mathematical models designed by experimental design strategy for biodiesel production from waste cooking oil using biomass-derived CaO catalyst.

1.6 Scope and Limitation of the Study

One of the main focuses of this research is the characterisation of the biomass-derived catalyst for the production of biodiesel. First of all, the potential of biomass to produce the desired catalyst is investigated. Then, the mechanisms involved in biodiesel production are studied. After that, the synthesised catalysts from the selected biomass are examined through various characterisation tests to inspect the structure and properties of the synthesised catalysts. The catalyst is then applied to biodiesel production to investigate its catalytic performance.

Next, there are a few parameters that affected the production of biodiesel. The effect of the parameters and interaction between the parameters are analysed based on the mathematical models designed by experimental design strategy. In addition, the optimum operating conditions for biodiesel production with the use of biomass-derived catalysts are determined as well.

CHAPTER 2

LITERATURE REVIEW

2.1 Heterogeneous Catalysts

Homogeneous catalysts and heterogeneous catalysts are commonly used in the biodiesel production process. Homogeneous catalysts are catalysts that exist in the same phase as the reactants while heterogeneous catalysts are not in the same phase as the reactants. Heterogeneous catalysts are also known as solid catalysts. Compared to homogeneous catalysts, heterogeneous catalysts are preferred in biodiesel production because they can be separated easily from the biodiesel mixture. This simplified the purification process considerably and reduced the wastewater generation as no product washing is needed to meet the biodiesel standard (Diamantopoulos, 2015). Furthermore, heterogeneous catalysts have a high chance of being reused and therefore significantly reduce the cost of production. Although homogeneous catalysts can catalyse the reaction under mild conditions to achieve a high yield of biodiesel within a short period, the catalysts often cause corrosion in the equipment parts (Atadashi, et al., 2013). Hence, heterogeneous catalysts are commonly used as they can reduce corrosion problems.

Heterogeneous catalysts are also effective in accelerating the transesterification process even though in the presence of FFA and water, which then ensure a rapid separation of pure glycerol from the biodiesel mixture and thus simplify the purification process (Panpraneecharoen, Punsuvon and Puemchalad, 2015). Next, it is vital to keep the moisture content of the biodiesel production process as low as reasonably practicable to avoid the formation of FFA through the hydrolysis of the ester by water. Thus, heterogeneous catalysts have emerged as a great catalyst for biodiesel production as they can overcome the drawbacks of homogeneous catalysts.

2.1.1 Basic Catalyst

Most of the biodiesel production processes in the industry have employed heterogeneous base catalyst in the transesterification reaction as it provides a higher rate of reaction as compared to the heterogeneous acid catalyst (Lam,

Lee and Mohamed, 2010). Next, it can be operated under relatively mild conditions such as low temperature and pressure are needed for the heterogeneous base catalyst to ensure a high conversion yield of biodiesel up to 98 % (Kar, Gupta and Das, 2012). The other beneficial properties of the heterogeneous base catalyst are long life-time, reusable and can be separated easily from the product.

However, the heterogeneous base catalyst is sensitive to FFA and water contents in the oils attributed to its basic characteristic. If the content of FFA in the oil exceeds 2 wt. %, this will result in soap formation which reduces the yield of biodiesel and causes catalyst deactivation (Kouzu, et al., 2007). Hence, a heterogeneous base catalyst is mainly applicable for biodiesel production from high-quality feedstock with low FFA content such as vegetable oil. Agarwal, et al. (2011) stated that a heterogeneous base catalyst has poor stability as its catalytic activity declines after three cycles of the reaction, resulting in low biodiesel yield. In addition, the heterogeneous base catalyst may become toxic when contacted with the ambient air.

Alkaline earth metal oxides such as magnesium oxide, beryllium oxide and calcium oxide (CaO) are common examples of the heterogeneous base catalyst. CaO catalyst performs well in the biodiesel production process. A biodiesel yield of 99 % was obtained in a reaction time of 1.25 hours by using 3 wt. % of CaO catalyst at 65 °C and 6:1 methanol to vegetable oil molar ratio (Colombo, Ender and Barros, 2017). Next, Atadashi, et al. (2013) showed that by using 8 wt. % of CaO catalyst, the yield of biodiesel is over 95 % and a purity of 93 % was obtained in a reaction time of 3 hours. This study was performed at 65 °C with 12:1 alcohol to the soybean oil molar ratio.

Besides that, Lam, Lee and Mohamed (2010) used potassium phosphate as catalyst to generate biodiesel in their studies. The FAME yield was reported to reach 97.3 % when 6:1 methanol to oil molar ratio was used. The other operating parameters such as the operating temperature of the reaction and reaction time were set at 60 °C and 2 hours, respectively.

2.1.2 Acid Catalyst

Compared to the heterogeneous base catalyst, a heterogeneous acid catalyst is more effective to deal with the feedstock with high FFA content as it is

insensitive to FFA. It can catalyse the esterification and transesterification processes simultaneously without the formation of soap, which eliminates the need for the pre-treatment step to convert the FFA (Atadashi, et al., 2013).

Next, the stability of the heterogeneous acid catalyst is high. It can handle FFA during biodiesel production without catalytic deactivation (Kouzu, et al., 2007). Thus, the heterogeneous acid catalyst is widely applied in the production of biodiesel from low-grade oils which consist of a high FFA level. Furthermore, the heterogeneous acid catalyst is recyclable, easy to separate from the product and reusable.

Due to its low reaction rate, heterogeneous acid catalyst requires high reaction conditions to produce biodiesel with high conversion yield (Leung, Wu and Leung, 2010). For example, high operating temperature and pressure, long reaction duration and high methanol to oil molar ratio are needed during the heterogeneous acid-catalysed reaction. This will lead to high energy requirements. The cost of the heterogeneous acid catalyst is higher than the basic catalyst because its synthesising process is quite complicated (Lam, Lee and Mohamed, 2010). Next, product contamination may occur due to the leaching problem of the solid acid catalyst.

Several examples for the heterogeneous acid catalyst used in biodiesel production are sulphonated zirconia, tungsten oxides and carbon-based solid acid catalysts. Guldhe, et al. (2017) used 15 wt. % of tungstate zirconia solid acid catalyst in the biodiesel production from microalgal lipids. They obtained 94.58 % of biodiesel yield at a high temperature of 150 °C and methanol to oil molar ratio of 12:1.

Lam, Lee and Mohamed (2010) obtained 91.5 % of FAME yield from waste frying oil in a 3 hours reaction by using sulphated tin oxide catalyst. The reaction was performed at 150 °C with the catalyst loading of 6 wt. % and alcohol to oil ratio of 30:1. Besides that, FAME yield of 92.1 % was achieved in 8 hours by using 10 wt. % of carbon-based heterogeneous acid catalyst at 80 °C and methanol to waste cooking oil molar ratio of 30:1 (Guan, Kusakabe and Yamasaki, 2009). Therefore, the heterogeneous acid catalyst has been proven as an effective catalyst for treating high FFA feedstocks in the biodiesel production process.

2.2 Biomass Derived Catalyst

A significant amount of biomass waste has been produced by every country each year but most of them are burned or ended in the landfill. The utilisation of biomass waste is a quite challenging topic. In the past few years, groups of researchers utilized biomass waste to synthesise catalysts and they found out that the biomass-derived catalysts possess high catalytic activity and clear textural characteristics (Wei, et al., 2019). This discovery provides a solution for reducing the biomass waste issue. Catalyst derived from biomass has gained popularity in the last few years as it has high catalyst stability. The catalyst synthesised and derived from biomass is also known as a green catalyst. This type of catalyst is environmentally friendly and cheap compared to those conventional catalysts since it is biodegradable and made from a low-cost substance which is biomass.

Biomass is an organic matter with carbon-based and also composed of other elements. The carbon in the biomass is absorbed from the surrounding in the form of carbon dioxide. The implementation of biomass waste as a feedstock for the preparation of heterogeneous catalysts is a promising method in biodiesel production as the biomass is abundantly available. The biomass-derived heterogeneous catalysts can be synthesised through carbonisation process which will be discussed later in the subsequent section.

Huge quantities of biomass waste offer a wide variety of sources for catalyst preparation. Table 2.1 outlines some biomass-derived solid catalysts for biodiesel production. Among the biomass source, waste shells such as eggshells have been widely investigated as a solid catalyst for the production of biodiesel and offer a high biodiesel yield. Large amounts of waste eggshells are generated daily, especially in the food industry. The eggshell is formed by carbonate which consists of oxygen and carbon atoms. It is enriched with calcium carbonate (CaCO_3) which will be decomposed to CaO at high temperatures during the carbonisation process (Abdullah, et al., 2017). CaO is a type of promising catalyst as it exhibits good catalytic performance, non-toxic and good catalyst stability. Hence, the CaO catalyst could be a viable choice for the production of biodiesel.

Table 2.1: Biomass-Derived Solid Catalysts Used in Biodiesel Production.

Type of Biomass	Feedstock	Calcination Temperature (°C); Time (h)	Esterification & Transesterification Conditions				FAME Yield (Y) or Conversion (C) (%)	Reference
			Methanol to Oil Molar Ratio	Temperature (°C)	Time (h)	Catalyst Loading (wt. %)		
Chicken Eggshell	Palm oil	900;4	9:1	60	4	20	94.4	(Abdullah, et al., 2017)
Duck Eggshell	Soybean oil	900;4	10:1	60	1.3	15	94.6	(Yin, et al., 2016)
Scallop Waste Shell	Karanja oil	1000;4	9:1	65	3	10	95.4	(Buasri, et al., 2014)
Coconut Hush Ash	Jatropha oil	500;1	12:1	45	0.5	7	90.0	(Vadery et al., 2014)
Sugarcane Bagasse	Waste cooking oil	600;2	18:1	65	5	10	94.4	(Zhang, et al., 2014)

2.2.1 Carbonisation of Biomass

Carbonisation of biomass refers to the process where the biomass is heated to a certain temperature over a specific period of time to produce a porous carbon-enriched solid. This process can be done by a few common methods which are template-directed synthesis method, hydrothermal carbonisation and direct synthesis method.

In the template-directed synthesis method, the template made up of nanoporous material is applied to form the porous carbonaceous substances. The carbonaceous substances formed have a well-distributed pore size directed by the template during the carbonisation process which strengthens the structural order (Deng, Li and Wang, 2016). The template used can be a soft template or a hard template. Both will give the same result in the formation of carbon materials. The major drawback of this method is the carbonaceous structure formed may crumble at extreme temperatures after being detached from the template.

Hydrothermal carbonisation can be divided into high temperature processes and low temperature processes. The high-temperature hydrothermal carbonisation process is performed under either superheated steam or supercritical water at a high temperature that exceeds 300 °C. The carbonisation process under supercritical water is preferred as it can penetrate into the pore structure at a fast rate to produce highly porous carbonaceous materials with a large surface area (Titirici, et al., 2007). The low-temperature hydrothermal carbonisation process is carried out at temperature up to 250 °C and it is less energy extensive if compared to the high-temperature method. However, it is a complex process as different soluble products may be generated while handling the carbon materials.

The direct synthesis carbonisation method is generally performed at a temperature between 300 °C to 1000 °C. Structures formed within this temperature range are found to have superb pore size and volume. Without the need for the template and supercritical water, the direct synthesis carbonisation method is capable to produce ordered mesoporous carbon materials from starting materials with low surface area (De, et al., 2015). Furthermore, it is environmentally friendly and easy to perform as no complicated procedure is involved.

Another process that is similar to carbonisation is calcination. Both of them are thermal treatment processes used in the preparation of biomass-derived solid catalysts which provide good catalytic activity. Moreover, both processes operate at a temperature between 300 °C and 1000 °C (Wang, Yan and Zhao, 2019). During combustion, CaCO_3 in the organic matter will decompose into CaO and produce carbon dioxide gas. The carbonisation temperature and calcination temperature are key factors in determining the catalyst performance as well as the catalyst's surface morphology. The formation of CaO is strongly affected by the temperature and it provides additional voids on the carbon structure which in turn leads to high catalytic activity due to the increasing pore diameter and pore volume (Abdullah, et al., 2017).

Smith, et al. (2013) reported that the catalyst's performance is dependent on the carbonisation temperature. Based on the study, the carbon catalyst prepared from bovine bone waste at a carbonisation temperature range from 350 °C and 550 °C showed no significant effect on FAME yield. This may be due to insufficient energy for the formation of porous carbon structures at low temperatures. Next, increasing the carbonisation temperature from 650 °C to 950 °C displayed an increase in catalytic activity which in turn improves the FAME yield. However, at a temperature higher than 950 °C, the catalytic performance declined significantly. This may be due to the thermal decomposition of the carbon structure at excessive temperature and the presence of micro-pores that reduce the number of active sites.

On the other hand, another research done by Geng, et al. (2012) showed that the carbon content in the catalyst sample increases with increasing carbonisation temperature. This finding also confirmed the effect of carbonisation temperature on catalytic performance. However, the optimum carbonisation temperature varies between different catalysts. It is dependent on the feedstock used to prepare the biomass-derived catalyst.

Apart from carbonisation temperature, carbonisation time is also another factor to be considered. Dawodu, et al. (2014) stated that incomplete carbonisation is preferred as this will lead to the gradual dehydration of carbon materials which resulted in the formation of aliphatic carbon structure and amorphous polycyclic aromatic. According to the results obtained, a higher

amount of smaller carbon sheets was formed and a higher specific surface area was recorded at the carbonisation time of 1 hour compared to the carbonisation time of 5 hours, which reported a higher catalytic performance.

Another study was done by Liu, et al. (2013) to study the influence of carbonisation temperature and carbonisation time on the ester yield. As shown in Figure 2.1, the results illustrated that the catalyst prepared from corn straw at a carbonisation time of 1 hour reported the highest ester yield. Further increment in the carbonisation time caused a decline in ester yield. This finding matched with the results obtained by Dawodu, et al. (2014). Next, the optimum carbonisation temperature for the corn straw-based catalyst is found to be at 573 K. The catalytic performance and ester yield declined significantly at a temperature higher than 600 K due to the carbon structure disintegrated at excessive temperature.

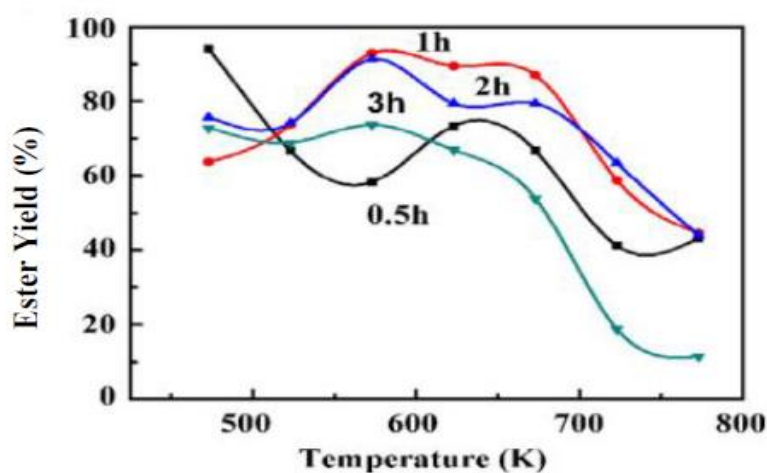


Figure 2.1: Effect of Carbonisation Time and Carbonisation Temperature on Ester Yield (Liu, et al., 2013).

As compared to carbonisation temperature, carbonisation time was found to have less impact on the catalytic performance. The study done by Wong, et al. (2020) showed that an increase in carbonisation time from 1 hour to 4 hours only resulted in very minor changes in the FAME yield. However, prolonged carbonisation time caused a noticeable decline in the FAME yield. The results obtained are summarised in Figure 2.2. On the other hand, large changes were reported in the FAME yield when the carbonisation temperature

rose from 400 °C to 800 °C as shown in Figure 2.3. The findings implied that carbonisation time had no significant influence on the biomass-derived catalysts' structure.

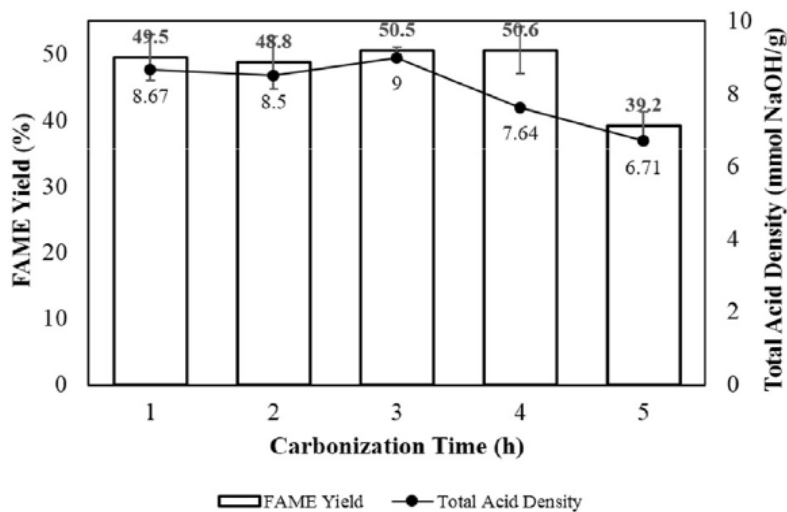


Figure 2.2: Effect of Carbonisation Time on FAME Yield and Total Acid Density of Prepared Catalyst (Wong, et al., 2020).

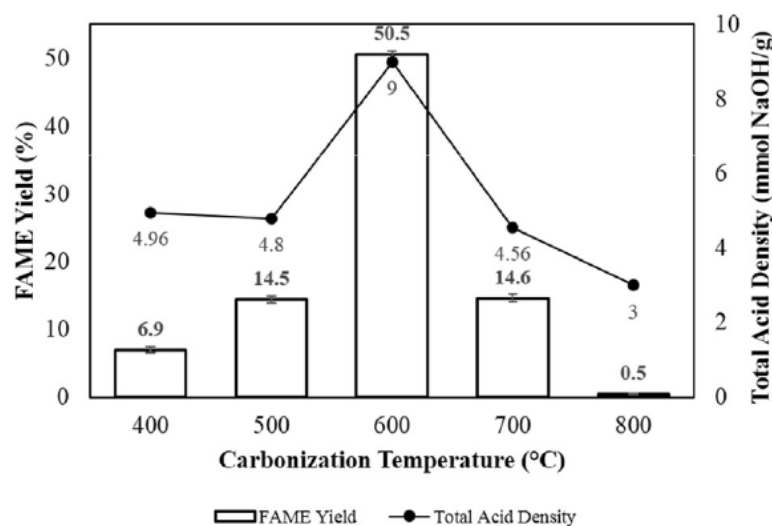


Figure 2.3: Effect of Carbonisation Temperature on FAME Yield and Total Acid Density of Prepared Catalyst (Wong, et al., 2020).

As a conclusion, the catalyst performance is strongly dependent on the carbonisation temperature. However, it is also important that the carbonisation time should not be too long as prolonged carbonisation duration will degrade the catalytic performance and also the FAME yield.

2.2.2 Biomass Derived Calcium Oxide Catalyst

CaO is present in significant amounts in the world as it can be synthesised through different sources and methods. CaO is generally formed from the calcination of CaCO_3 at high temperatures. Several studies have been conducted to prepare CaO heterogeneous catalyst from a variety of biomass sources such as chicken eggshell, mussel shell, snail shell, ostrich eggshell and scallop shell. The studies have shown that the CaO catalyst derived from biomass exhibited great catalytic performance and high tolerance of oil with high FFA content.

A study was done by Boey, Maniam and Hamid (2011) to investigate the effect of CaO solid catalyst derived from chicken eggshell on the transesterification of waste cooking oil with high FFA content (6.6 %). The CaO catalyst was prepared by calcinating the crushed chicken eggshell at temperature of 800 °C in a furnace for 24 hours to ensure a complete decomposition of CaCO_3 to form CaO. From the result obtained, 90 % of biodiesel yield was achieved, which was considerably high as compared to the use of conventional potassium hydroxide catalyst that yielded 61 % of biodiesel. A similar study was done by Sharma, Singh and Korstad (2011) and the results also showed a high biodiesel yield of 95 % with the use of chicken eggshell-derived CaO catalyst.

Buasri, et al. (2014) used Karanja oil that contained 3.2 % of FFA with CaO catalyst originated from scallop waste shell in their study. The scallop waste shells were calcined in a muffle furnace for 4 hours at 1000 °C. The biodiesel yield achieved was 95.4 %, with a catalyst loading of 10 wt. % and alcohol to oil molar ratio of 9:1 at 65 °C. In addition, Gendy, Deriase and Hamdy (2014) demonstrated the application of CaO catalyst produced from snail shells for the biodiesel production from waste frying oil. The catalyst was calcined at 800 °C. The result showed a 96 % of biodiesel yield within a reaction time of 1 hour.

All these studies revealed that the biomass-derived CaO catalyst can be utilised as a low-cost and environmentally friendly solid catalyst for biodiesel production.

2.3 Mechanism for Biodiesel Production

Two main mechanisms are involved in biodiesel production depending on the type of catalyst used. Base-catalysed transesterification reaction adopted the application of basic catalysts while acid-catalysed transesterification reaction adopted the application of acid catalysts.

2.3.1 Acid Catalysed Transesterification

The mechanism of acid-catalysed transesterification reaction is shown in Figure 2.4. The first stage (I) is the protonation of the ester's carbonyl group (I). This will lead to the formation of a carbocation (II). The carbocation formed is extremely reactive and it can undergo a competitive reaction to form carboxylic acids in the presence of water (Shin, et al., 2012). Therefore, water must be avoided during the transesterification reaction to prevent the occurrence of undesired reactions. Then, a tetrahedral intermediate (III) is formed as a result of the nucleophilic attack of alcohol to the carbocation (Deshpande, Sunol and Philippidis, 2017). Lastly, glycerol elimination occurs and a new ester (IV) is formed.

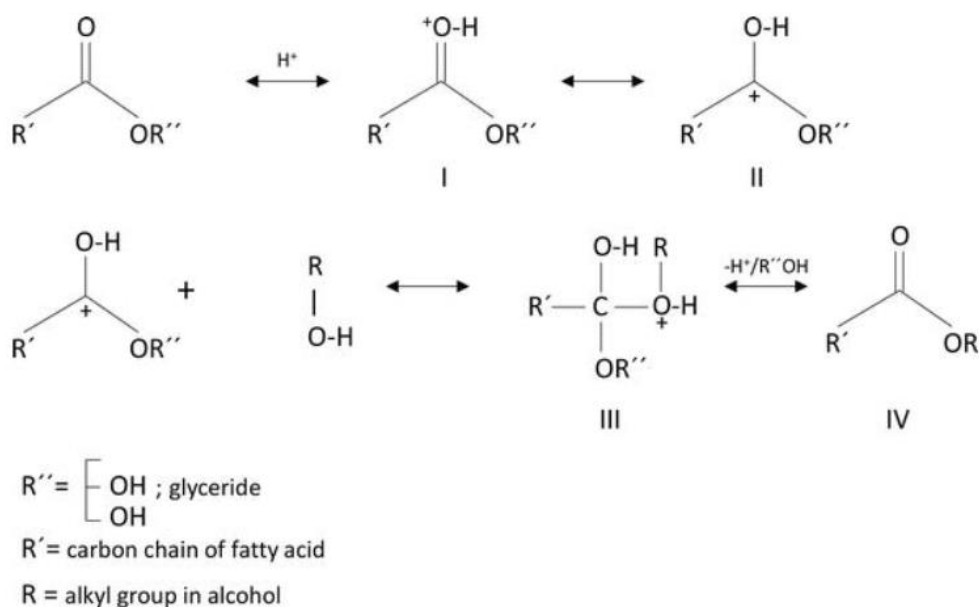


Figure 2.4: Mechanism of Acid Catalysed Transesterification (Deshpande, Sunol and Philippidis, 2017).

2.3.2 Base Catalysed Transesterification

The mechanism of base-catalysed transesterification is shown in Figure 2.5. When a basic catalyst is used, the reaction between the catalyst and alcohol will form an alkoxide ion (Deshpande, Sunol and Philippidis, 2017). Then, the alkoxide ion attacks the carbonyl carbon of the triglyceride. This will eventually lead to the formation of a tetrahedral intermediate as shown in step 1. During the second step, the reaction between the alcohol and the tetrahedral intermediate generates a new alkoxide ion (Meher, Vidyasagar and Naik, 2016). Lastly, the rearrangement of the intermediate results in the formation of a diglyceride and an ester.

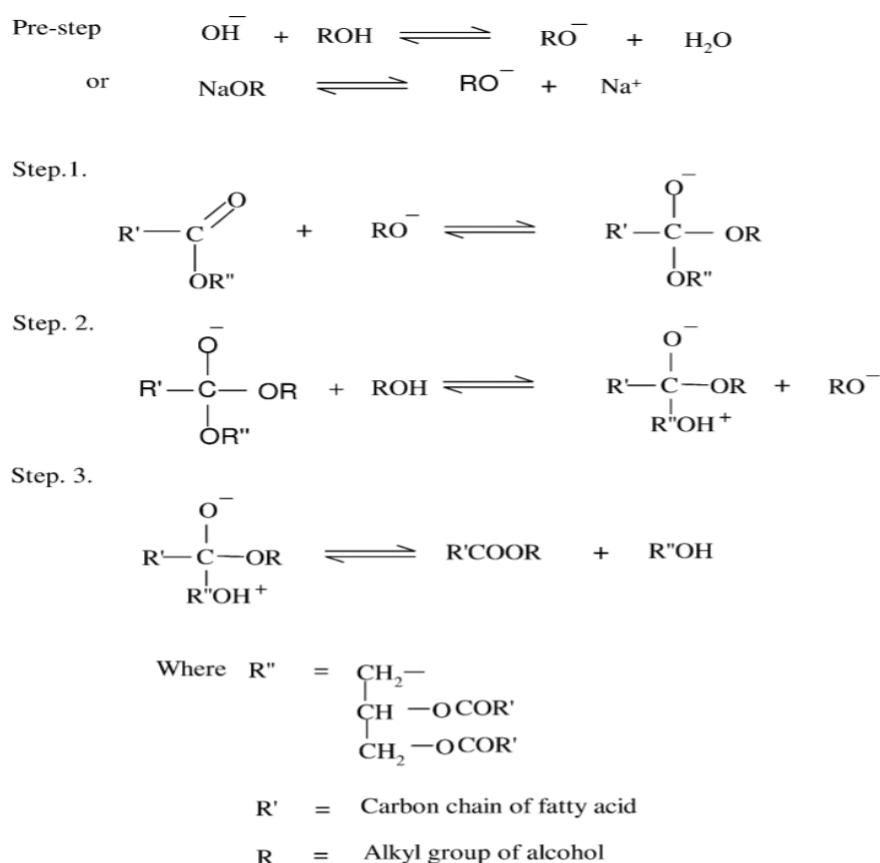


Figure 2.5: Mechanism of Base Catalysed Transesterification (Meher, Vidyasagar and Naik, 2016).

2.3.3 Calcium Oxide Catalysed Transesterification

The mechanism for the biodiesel production using CaO as the catalyst is described in Figure 2.6. In the first step, the oxide ion on the CaO catalyst surface extracts the hydrogen ion from the hydroxyl group of methanol and

forms methoxide ion (Boey, Maniam and Hamid, 2011). Then, the attachment of methoxide ion to the carbonyl carbon of the triglyceride molecule generates a tetrahedral intermediate (Bharti, et al., 2020). After that, the tetrahedral intermediate takes up the hydrogen ion on the CaO surface. Lastly, rearrangement of the tetrahedral intermediate leads to the formation of FAME. The reaction repeats for the diglycerides and monoglycerides. The overall reaction gives one mole of glycerol and three moles of FAME.

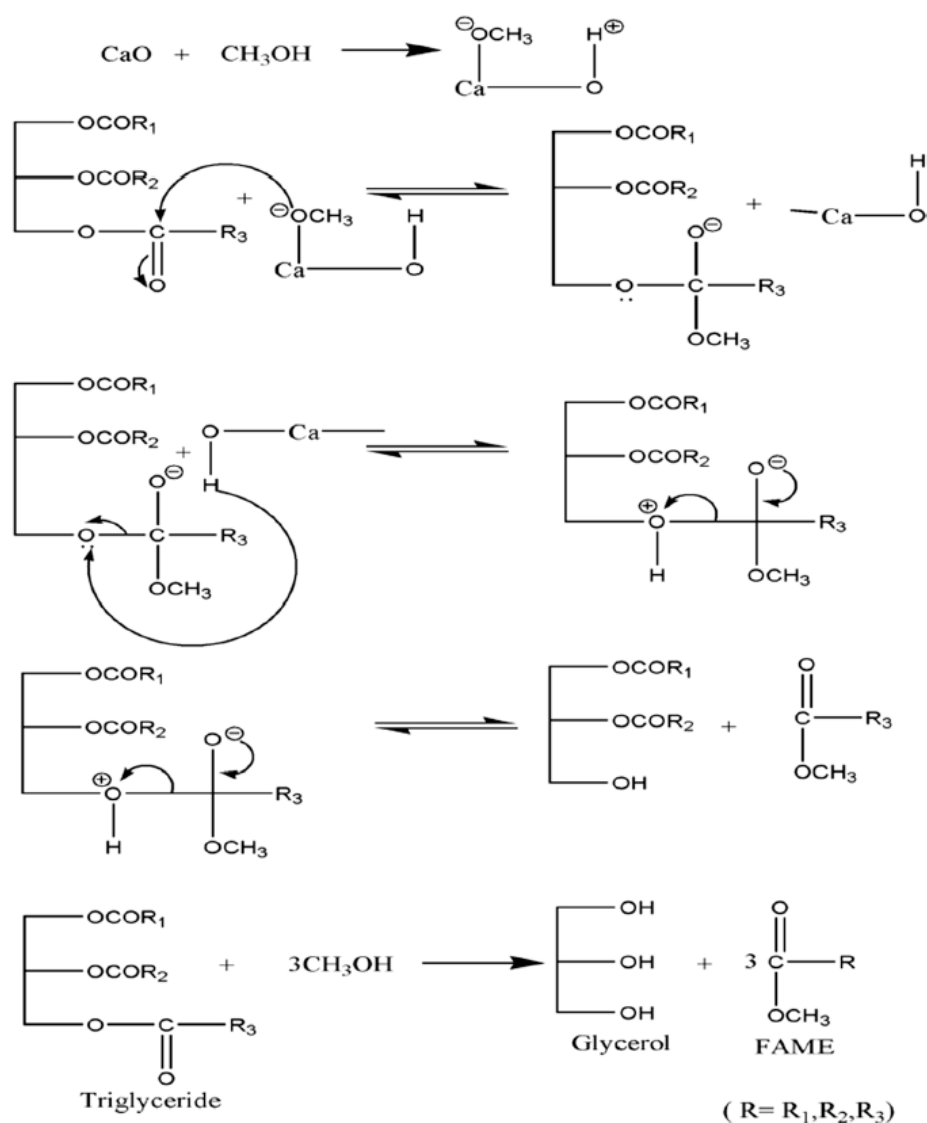


Figure 2.6: Mechanism of CaO Catalysed Transesterification (Bharti, et al., 2020).

2.4 Operating Parameters that Affect Biodiesel Production

The operating parameters that affect biodiesel production include the reaction time, alcohol to oil molar ratio, temperature of reaction and catalyst loading. It is important to study these parameters to achieve a desired biodiesel yield and also ensure sustainable biodiesel production.

Alcohol acts as a reactant and portrays a crucial role in biodiesel production. Methanol is commonly used as it is easily available and low cost. From the stoichiometric equation of esterification reaction, alcohol reacts with a fatty acid in a molar ratio of 1:1 to produce one mole of FAME and water. For transesterification reaction, alcohols react with triglyceride in a ratio of 3:1 to generate three moles of FAME and one mole of glycerol. As both reactions are reversible, excess alcohol is needed to shift the reactions toward the forward direction (Shuit, et al., 2012). The research done by Maceiras, et al. (2009) showed the FAME yield increased by 40 % when the methanol to waste frying oil molar ratio raised from 1:1 to 25:1. Next, Gupta and Rathod (2019) reported that the biodiesel yield increased with raising alcohol to oil molar ratio from 5:1 to 10:1. The optimum ratio in this study was found to be 8:1 which resulted in 96.81 % of conversion. Further increment in the molar ratio caused no considerable changes in the conversion.

The temperature of the reaction is one of the significant factors that must be considered during biodiesel production. Generally, a higher reaction temperature will lead to a higher rate of reaction, resulting in high biodiesel yield. Liu, et al. (2008) investigated the effect of temperature on biodiesel production from soybean oil. The results depicted that the conversion of feedstock increased significantly as the temperature of the reaction increased from 30 °C to 65 °C. The optimum reaction temperature was reported at 65 °C, similar to the boiling point of methanol. Further increment in reaction temperature above 65 °C led to a rapid drop in the soybean oil conversion. This may probably be due to the vaporisation of methanol at the temperature of 65 °C which led to the bubble formation. The bubbles disrupted the reaction and caused a decline in the rate of reaction.

Degfie, Mamo and Mekonnen (2019) studied the effect of reaction time on the biodiesel yield by keeping other parameters constant on their optimum value. It was reported that the biodiesel yield increased from 68 % to 96 % when the reaction time prolonged from 30 minutes to 90 minutes. However, the biodiesel yield dropped as the reaction extended to 140 minutes. This indicated that a longer reaction time will only result in a higher biodiesel yield before the chemical equilibrium is reached. Further extension of the reaction time beyond the optimum reaction time caused the reaction to shift towards the backward direction and reduced the biodiesel yield. Furthermore, the reaction time needed was strongly dependent on other parameters such as the temperature of the reaction and the alcohol to oil molar ratio. According to Villa, et al. (2010), the increase in reaction temperature and alcohol to oil molar ratio led to higher catalyst activity and also a higher reaction rate, which greatly reduced the time needed to reach the optimum yield or conversion.

Next, the influence of catalyst loading on biodiesel production was studied by Gupta and Rathod (2019). They found out that the FAME yield increased with increasing catalyst loading from 0.5 wt. % to 1.5 wt. %. High methanol to oil ratio may lead to a mass transfer problem. Hence, high catalyst loading is needed to accomplish the complete conversion. Another research done by Tremblay, Cao and Dubé (2008) showed that 100 % conversion of oil was achieved in 20 minutes reaction time at a catalyst loading of 0.5 wt. % while only 61.1 % of conversion of oil was achieved at a catalyst loading of 0.05 wt. %. It was still capable to achieve 100 % conversion at low catalyst loading but it took a longer reaction time to reach it. Degfie, Mamo and Mekonnen (2019) showed that the biodiesel yield increased when the catalyst loading increased. The reaction reached a maximum yield of 96 % at 1 wt. % catalyst loading. However, the biodiesel yield declined to 80 % at a catalyst loading of 5 wt. %. This was due to the excessive amount of catalysts that led to the formation of soap which hindered the reaction.

2.5 Response Surface Methodology

Experimental design portrays a crucial role in the areas of science and engineering as well as in some scientific studies. Generally, a process can be influenced by many factors or variables and some variables will have significant impact on the output of the process. It is vital to know the main parameters that affect the process and what the target level of those variables should be in order to obtain the optimal results. Without experimental design, experiments have to be performed in a way that one variable is being tested while the others remained constant. However, this generally requires a lot of time and testing to obtain the optimal results. Therefore, experimental design can be employed to solve these issues. The response surface methodology (RSM) is a frequently used experimental design for optimisation which can evaluate the impacts of multiple process variables and their interactions on the response variables (Saffari, 2018).

RSM has been adopted by many researchers in their studies regarding the production of biodiesel. Silva, Camargo and Ferreira (2011) optimised the levels of different process variables for biodiesel production from soybean oil by using RSM along with factorial design. The optimal levels of process variables were found to be 9:1 ethanol to oil molar ratio, 80 minutes reaction time, 1.3 M catalyst concentration and 40 °C reaction temperature, which resulted in 95 % biodiesel yield. In another study, Chumuang and Punsuvon (2017) employed RSM and reported that maximum biodiesel yield of 99.43 % can be achieved when the reactions were performed using 11.6:1 methanol to oil molar ratio and 2.83 wt. % catalyst concentration for 100.14 minutes. Next, RSM coupled with central composite design (CCD) has also been employed by Yuan, et al. (2008) for the optimised biodiesel production from waste oil. The researchers reported 83.34 % biodiesel yield using a catalyst loading of 1 wt. % and alcohol to oil ratio of 6.5:1 at 48.2 °C for 65.4 minutes. Furthermore, Salamatinia, et al. (2010) and Tan, et al. (2017) also applied RSM to examine the optimal levels of reaction parameters for the biodiesel production from palm oil and waste cooking oil respectively.

2.5.1 Design Strategy for RSM

The selection of a suitable design strategy is important in the application of RSM as it exerts a great influence on the construction of the response surface and also the accuracy of the predicted model (Saffari, 2018). The common design strategies used in RSM are full factorial design (FFD), Box-Behnken design (BBD), central composite design (CCD) and Doehlert design (DD). The common software used are Design Expert and MATLAB.

FFD comprises all possible combinations of the levels for all input factors, where all factors are typically set at two or three levels (Ochkin, Gladilov and Nekhaevskiy, 2012). In two-level FFD, each input variable takes on two values, which are low (-1) and high (+1) values and the number of runs will be $2k$ when there are k factors. The three-level FFD considers three values which are low (-1), central (0) and high (+1) values. Then, the number of designs will be 3^k when there are k variables. Three-level FFD is more common compared to the two-level FFD. However, more experimental runs are needed for the 3^k design, which generates unwanted high-order interactions. Hence, according to Karimifard and Alavi (2018), the three-level FFD will be more suitable if there are less than five factors.

CCD is the most well-known fractional factorial design that is suitable for fitting second-order or quadratic polynomial models. In CCD, each factor or variable requires five levels which are -1, 0, +1, $-\alpha$ and $+\alpha$. CCD consists of three types of design points: cube points which are expressed as -1 and +1, center points which are expressed as 0 and axial points which are expressed as $-\alpha$ and $+\alpha$. The axial points are employed to improve the readability level of the model while the center points are applied to measure the experimental error (Behera, et al., 2018). CCD can provide maximum information with the least number of runs, but it is quite time-consuming if a great number of factors are involved (Bhattacharya, 2021).

Next, BBD is a three-level incomplete factorial design that is restricted solely to the building of second-order polynomial models. It is said to be more efficient than the three-level FFD and slightly efficient than CCD. According to Ferreira, et al. (2007), extreme conditions in the experiments that may lead to unsatisfactory results can be avoided by using BBD as all the factors in this design are at their lowest or highest levels simultaneously. Conversely, BBD is

not applicable if the responses at extreme conditions must be known. Another limitation of BBD is there must be a minimum of three experimental factors for the design to work (Karimifard and Alavi, 2018).

Then, DD is a flexible design method in which each variable can have a different number of levels. This feature is quite important especially when some factors are subject to restrictions. Although DD is not as common as CCD and BBD, it provides fewer experimental runs even with a large number of factors (Quintella, et al., 2004).

2.5.2 Model Fitting and Analysis

After the selection of the suitable design strategy, the obtained mathematical model must be fitted to the experimental data in order to depict the performance of the response. Generally, first-order model is applied for depicting a flat surface based on low degree polynomial model. The equation for the first-order model is shown in Equation (2.1).

$$R = b_o + \sum b_i X_i + \sum b_{ij} X_i X_j + e \quad (2.1)$$

A more structured second-order model is used to determine the optimum point if the first-order models are not sufficient to express the true functional relationships of the variables (Sakkas, et al., 2010). The equation for the second-order model is shown in Equation (2.2).

$$R = b_o + \sum b_i X_i + \sum b_{ij} X_i X_j + \sum b_{ii} X_i^2 + e \quad (2.2)$$

where

R = response value

b_0 = coefficient of the constant term

b_i = coefficients of the linear terms

X = input variables

b_{ij} = coefficients of the interaction terms

b_{ii} = coefficients of the quadratic terms

e = error term

Then, the contour plots of the response can be obtained. This three-dimensional response surface plot can help to visualise the influence of the input variables on the response and also the interaction effects between the variables (Lorza, et al., 2018). The accurateness of the model can then be determined by examining the coefficient of determination (R^2) and analysis of variance (ANOVA). According to Karimifard and Alavi (2018), R^2 should be assessed alongside with the predicted R^2 , adjusted R^2 and the residual plots to examine the adequacy of the regression model because a high R^2 does not really represent that the model is fit. Next, the significant factors that greatly influence the response of the model can be determined by ANOVA. A factor is said to be significant if its calculated probability or p -value is less than 0.05.

2.5.3 Optimisation

Optimisation is a process of determining the appropriate factor levels that give the best desired output by adjusting the variables in the process (Sakkas, et al., 2010). It is notable that there must have a highest and lowest level specified for all the factors and response. Then, the goals set for the input factors and response of the model can be target, minimise, maximise or within a certain range. For the current study, the objective of optimisation is to maximise the yield of the biodiesel by adjusting the levels of input factors within the specified range. The optimum solutions given by the RSM would generally compare with the experimental values to verify the validity of the predicted model. In this case, experiments are conducted under the optimised conditions and the results obtained will be compared with that of the predicted model. The developed model can be considered as a valid and robust design if the optimum solutions obtained are in agreement with the experimental results (Tan, et al., 2017).

CHAPTER 3

METHODOLOGY AND WORK PLAN

3.1 Documentary Analysis

The first part of this study involves the characterisation studies of the biomass-derived CaO catalyst for biodiesel production from waste cooking oil. After that, RSM was applied to evaluate the interaction between parameters for the production of biodiesel catalysed by the CaO catalyst generated from different biomass sources. A systematic analysis of the published works must be carried out in order to obtain reliable data and findings that are related to this study.

3.1.1 Searching for Related Published Works

The search for the relevant published works was performed across several comprehensive databases. The databases used in this study were Scopus, ScienceDirect, Google Scholar and UTAR Library databases. The searches only included the works published in English and from 2000 to 2020.

The selected search options for the Scopus database were “article title, abstract and keywords” while the search option for ScienceDirect, Google Scholar and UTAR Library databases was “keywords”. In this case, the keywords such as “biodiesel or FAME production”, “waste cooking oil”, “waste-derived calcium oxide catalyst”, “optimisation” and “response surface methodology” were chosen for the search in those databases. Then, those scientific articles or journals that related to the topic of this study were selected.

3.1.2 Study Selection and Data Collection

The selection of the published works obtained from the databases was based on several criteria. For instance, only works that relate to the production of biodiesel from waste cooking oil using biomass-derived CaO catalyst and works that reveal comprehensive results and systematic narrative reviews were selected. Published works that deal with the production of biodiesel by using other types of catalysts and feedstocks were then eliminated. This was done by

reviewing and evaluating the abstract of each works. Then, those published works that met the criteria were selected.

After that, the contents of the selected works were analysed accordingly. Then, data collection was conducted by extracting the qualitative and quantitative data that comprised relevant information to this study from the selected works such as the characterisation results of the synthesised catalysts, principles behind the findings and the optimum operating conditions for the biodiesel production. The data extracted were then reviewed and discussed appropriately.

3.2 Catalyst Characterisation Studies

The characterisation results of the biomass-derived CaO catalysts were discussed and analysed in this study which included the results obtained from Scanning Electron Microscopy with Energy Dispersive X-ray spectroscopy (SEM-EDX) analysis, Brunauer-Emmett-Teller (BET) surface area analysis, Thermogravimetric analysis (TGA), Fourier Transform Infrared spectroscopy (FTIR) analysis and X-ray diffraction (XRD) analysis.

SEM-EDX is a powerful technique that provides the surface topography, chemical composition and elemental information of the synthesised catalysts. High-resolution images of the catalysts can be obtained from SEM by scanning through the surface of the catalysts with the focused electron beam. The interactions between the catalysts sample and the electron beam generate signals that tell the morphology structure of the synthesised catalysts (Liu, et al., 2010). EDX is capable to detect the elements present in the sample by utilising the X-ray spectrum emitted from the interactions between the sample and the electron beam.

Next, the pore distribution and the surface area of the catalysts can be evaluated through BET surface area analysis. This analysis involves the adsorption of gas molecules on the sample surface at a low temperature which is about 77 K. Nitrogen is commonly used due to its powerful interactions with most of the solids. By calculating the amount of gas adsorbed on the monomolecular layer of the sample surface, the surface area of the sample can be determined (Titirici, et al., 2007). Then, the thermal stability of the catalysts

can be examined through TGA. It is done by measuring changes in the mass of the catalysts against time when the heat is supplied (Correia, et al., 2014).

FTIR is a rapid and non-destructive technique that provides information regarding the organic compounds present in the synthesised catalysts. It is usually applied to study the functional groups that exist in the catalysts. According to Omole and Dauda (2016), the sample absorbed the infrared radiation and at the same time transmitted some of the infrared radiation during the analysis. This created absorption or transmission spectrum that can identify the chemical bonds found in the catalysts.

On the other hand, XRD analysis is normally applied in the catalyst characterisation process to identify the compositions and the crystalline phases present in the catalysts. Diffraction occurs when the X-ray scattered from the sample surface undergoes constructive and destructive interference. The detection of constructive waves by the detector will generate an XRD spectrum and the identity of the solid structure can then be confirmed from the resulting diffractogram (Flores, et al., 2019). XRD is generally performed together with FTIR as the exact composition of the samples can be revealed accurately by this combination.

3.3 Response Surface Methodology for Calcium Oxide Catalysed Transesterification

RSM is a combination of statistical and mathematical methods that is beneficial for modelling, designing experiments, and process optimisation (Babaki, et al., 2017). RSM coupled with CCD in Design Expert was employed in this study to optimise the biodiesel production process and evaluate the impact of the process parameters on the biodiesel yield. As compared to the three-level FFD, CCD provides equal information but with fewer experiment runs (El-Gendy, Abu and Aziz, 2014). Furthermore, CCD is very useful in RSM for fitting a second-order or quadratic response surface model.

The production of biodiesel is mostly influenced by several process variables such as the reaction time, alcohol to oil molar ratio, catalyst concentration and the temperature of the reaction. From the published works selected, different combinations of these parameters were studied by different

researchers. The combined effect of these variables on biodiesel yield was modelled using Stat-Ease Design Expert version 12.0. Tables 3.1 to 3.5 show the range and levels of independent parameters used for the optimisation of biodiesel production from waste cooking oil by using different biomass-derived CaO catalysts.

Table 3.1: Range and Levels of the Process Parameters for Optimisation of Biodiesel Production Process that Involved Chicken Eggshell-Derived CaO Catalyst (Tan, et al., 2017).

Factors	Symbols	Units	-α	Low	Middle	High	+α
Methanol to oil ratio	A	-	6:1	8:1	10:1	12:1	14:1
Catalyst Concentration	B	wt. %	0.5	1.0	1.5	2.0	2.5
Reaction Time	C	h	0.5	1.0	1.5	2.0	2.5
Reaction Temperature	D	°C	35	50	65	80	95

Table 3.2: Range and Levels of the Process Parameters for Optimisation of Biodiesel Production Process that Involved Ostrich Eggshell-Derived CaO Catalyst (Tan, et al., 2017).

Factors	Symbols	Units	-α	Low	Middle	High	+α
Methanol to oil ratio	A	-	6:1	8:1	10:1	12:1	14:1
Catalyst Concentration	B	wt. %	0.5	1.0	1.5	2.0	2.5
Reaction Time	C	h	0.5	1.0	1.5	2.0	2.5
Reaction Temperature	D	°C	35	50	65	80	95

Table 3.3: Range and Levels of the Process Parameters for Optimisation of Biodiesel Production Process that Involved Snail Shell-Derived CaO Catalyst (Gendy, Deriase and Hamdy, 2014).

Factors	Symbols	Units	- α	Low	Middle	High	+ α
Methanol to oil ratio	A	-	6:1	6:1	7.5:1	9:1	9:1
Catalyst Concentration	B	wt. %	6	6	9	12	12
Reaction Time	C	h	1	1	2	3	3

Table 3.4: Range and Levels of the Process Parameters for Optimisation of Biodiesel Production Process that Involved *Donax deltoides* Shell-Derived CaO Catalyst (Niju, Vishnupriya and Balajii, 2019).

Factors	Symbols	Units	- α	Low	Middle	High	+ α
Methanol to oil ratio	A	% (v/v)	55.18	62	72	82	88.82
Catalyst Concentration	B	wt. %	4.64	6	8	10	11.36
Reaction Time	C	min	99.55	120	150	180	200.45

Table 3.5: Range and Levels of the Process Parameters for Optimisation of Biodiesel Production Process that Involved *Malleus malleus* Shell-Derived CaO Catalyst (Rabia, et al., 2018).

Factors	Symbols	Units	- α	Low	Middle	High	+ α
Methanol to oil ratio	A	-	3:1	6:1	9:1	12:1	15:1
Catalyst Concentration	B	wt. %	0.5	1.0	1.5	2.0	2.5
Reaction Time	C	min	30	60	90	120	150

After keyed in all the factors, several runs were generated randomly by the software. The total number of runs generated was based on the formula as shown in Equation (3.1), where k is the number of factors, C is the center point's runs and N is the total number of runs.

$$N = 2^k + 2k + C \quad (3.1)$$

The collected experimental data from the published works were used to optimise the biodiesel yield. The results obtained were then analysed through RSM and regression analysis.

CHAPTER 4

RESULTS AND DISCUSSION

4.1 Analysis of Catalyst Characterisation Studies

The CaO catalysts under study were synthesised from different sources of biomass. Characterisation of synthesised catalysts is important as it provides essential information regarding the structure, composition, thermal stability and morphology of the catalysts. The characterisation of catalysts can be done with the aid of analytical techniques.

4.1.1 Scanning Electron Microscopy with Energy Dispersive X-ray Spectroscopy (SEM-EDX) Analysis

The SEM images for the catalysts derived from different biomass are shown in Figure 4.1. From Figure 4.1 (a) and Figure 4.1 (b), it can be observed that the raw chicken eggshell and raw ostrich eggshell were in irregular non-porous crystal form. After calcination at 1000 °C, the structure of the chicken eggshell and ostrich eggshell turned into porous-like structures and their particle sizes also decreased as observed in Figure 4.1 (c) and Figure 4.1 (d). Furthermore, the small particles merged together and formed agglomerates after calcination. These observations are in accordance with the SEM results of the calcined *Donax deltoides* shell and calcined *Malleus malleus* shell as shown in Figure 4.1 (e) and Figure 4.1 (f) respectively. This was due to the changes in the structure of isolated isotropic CaO particles after calcination at high temperatures (Reddy, et al., 2017). According to Buasri, et al. (2014), the changes of the structure might due to the decomposition of CaCO₃ in the eggshell into CaO and carbon dioxide after the calcination process, which resulted in the decrement of the particle sizes. The results indicated that calcination process promoted the formation of porous structure which could provide a greater surface area to enhance the catalyst activity.

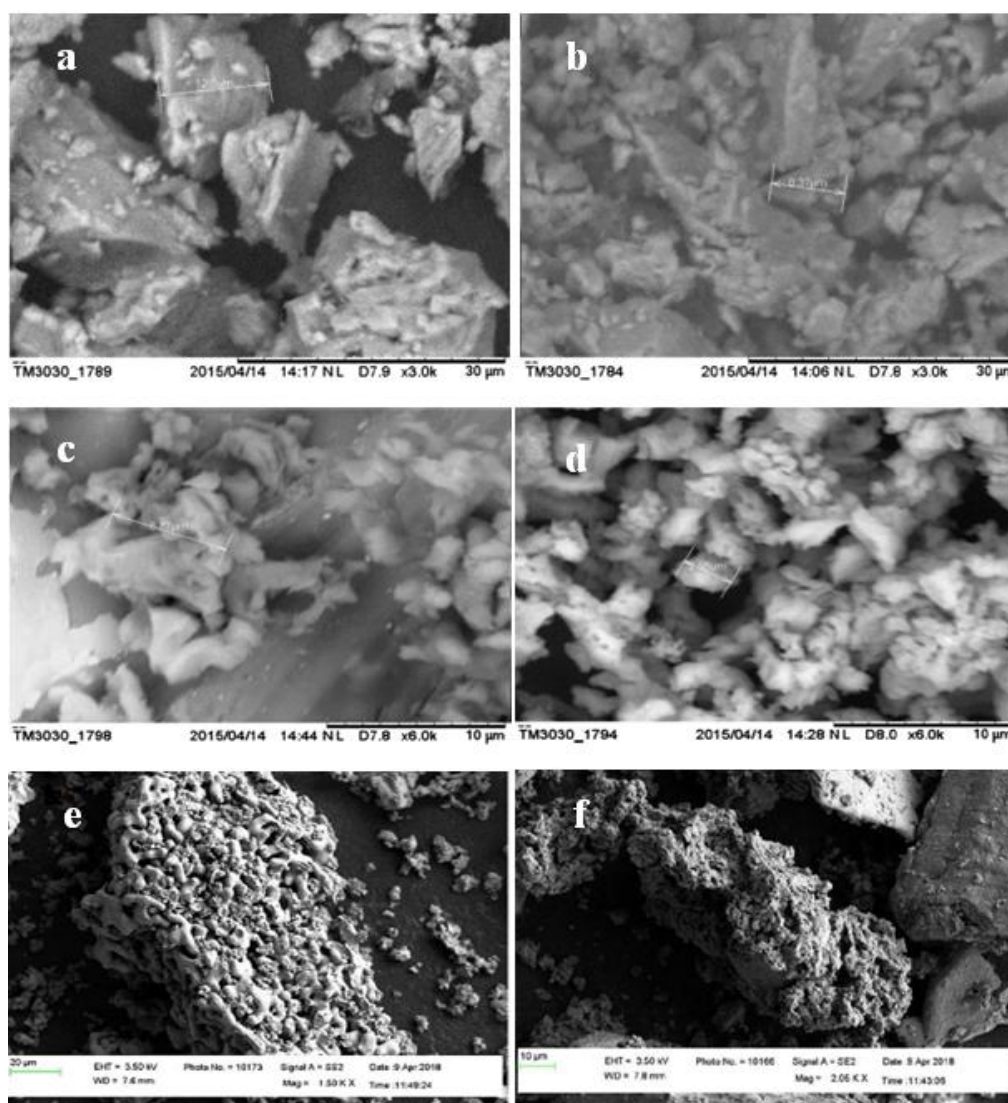


Figure 4.1: SEM Images of (a) Uncalcined Chicken Eggshell (Bharti, et al., 2020), (b) Uncalcined Ostrich Eggshell (Tan, et al., 2015), (c) Calcined Chicken Eggshell (Bharti, et al., 2020), (d) Calcined Ostrich Eggshell (Tan, et al., 2015), (e) Calcined *Donax deltoideis* Shell (Niju, Vishnupriya and Balajii, 2019) and (f) Calcined *Malleus malleus* Shell (Rabia, et al., 2018).

Next, the EDX results reported by Rabia, et al. (2018), Niju, Vishnupriya and Balajii (2019), Sun, Sage and Sun (2017) and Chaiyut, et al. (2013) revealed that CaO was the major phase present in the calcined *Malleus malleus* shell (98.31 %), calcined *Donax deltoideis* shell (99.16 %), calcined shrimp shell (70.60 %) and calcined cockle shell (99.17 %). This confirmed that the CaCO_3 in the raw samples has been decomposed into CaO upon calcination.

4.1.2 Brunauer-Emmett-Teller (BET) Surface Area Analysis

Table 4.1 shows the summary of the results of various biomass-derived CaO catalysts through BET analysis. Compared to the pure CaO and the uncalcined biomass sources, a larger surface area and larger pore volume were observed for all the CaO catalysts generated from the calcination of various biomass sources. The results revealed that the calcined ostrich eggshell possesses the highest BET surface area of 71.0 m²/g. Calcined bottom ash exhibited the lowest BET surface area might probably due to the low calcination temperature as the surface area would generally increase when the calcination temperature is increased. The increased in surface area after the calcination process might probably due to the formation of new pores during the decomposition of organic templates at high temperatures (Amadine, et al., 2017). Next, the formation of pores at high temperatures was ascribed to the evolution of gaseous water molecules from the catalyst, which further led to the increment in surface area and enhancement of the catalytic activity (Chaiyut, et al., 2013). The results from BET analysis showed that the calcination process would result in a strong increase of the catalyst's active site that promoted the interaction between the alcohol and catalyst in the reaction mixture (Chakraborty, et al., 2016).

4.1.3 Thermogravimetric Analysis (TGA)

From the studies conducted by different researchers, it was found out that the catalyst samples prepared from different types of biomass experienced two stages of weight loss during the thermal treatment. During the first stage, the samples experienced a minor weight loss at a temperature around 150 °C to 450 °C. According to Erhan and Singh (2007), the slight weight loss was due to the removal of absorbed moisture and organic compounds from the samples upon heating. During the second stage, a large weight loss was observed at a temperature around 600 °C to 850 °C. This significant weight loss was ascribed to the decomposition of CaCO₃ in the samples into CaO together with the release of carbon dioxide (Piker, et al., 2016). After these two stages, further increment in the temperature showed no weight loss in the samples which could be indicated that the CaCO₃ was completely decomposed to produce CaO and carbon dioxide (Roschat, et al., 2016).

Table 4.1: BET Surface Area and Pore Volume of Various Biomass-Derived CaO Catalysts.

Biomass	Calcination Temperature (°C); Time (h)	BET Surface Area (m ² /g)		Pore Volume (cm ³ /g)		References
		Uncalcined	Calcined	Uncalcined	Calcined	
Pure CaO	-	36.8	-	0.0126	-	(Tan, et al., 2015)
Chicken Eggshell	1000;4	1.9	54.6	0.0006	0.0148	(Tan, et al., 2015)
Ostrich Eggshell	1000;4	4.0	71.0	0.0009	0.0218	(Tan, et al., 2015)
Duck Eggshell	900;4	2.1	67.2	0.0006	0.0164	(Yin, et al., 2016)
Snail Shell	900;4	2.7	53.3	0.0017	0.0312	(Laskar, et al., 2018)
Bottom Ash	700;4	-	49.1	-	0.0653	(Maneerung, Kawi and Wang, 2015)
Cockle Shell	1000;4	-	59.87	-	0.0870	(Chaiyut, et al., 2013)

For example, Figure 4.2 illustrates the TGA result of the catalyst sample prepared from chicken eggshells. It could be observed that the chicken eggshell sample experienced a minor weight loss (8 %) at around 200 °C to 450 °C. Then, 37.2 % of weight loss was observed at a temperature around 640 °C to 740 °C. The TGA curves remained constant at a temperature range above 750 °C. This revealed that a higher temperature of above 750 °C would be better for the complete calcination of the chicken eggshell to convert CaCO_3 to CaO (Fayyazi, et al., 2018). Table 4.2 summarises the TGA data obtained for different catalyst samples.

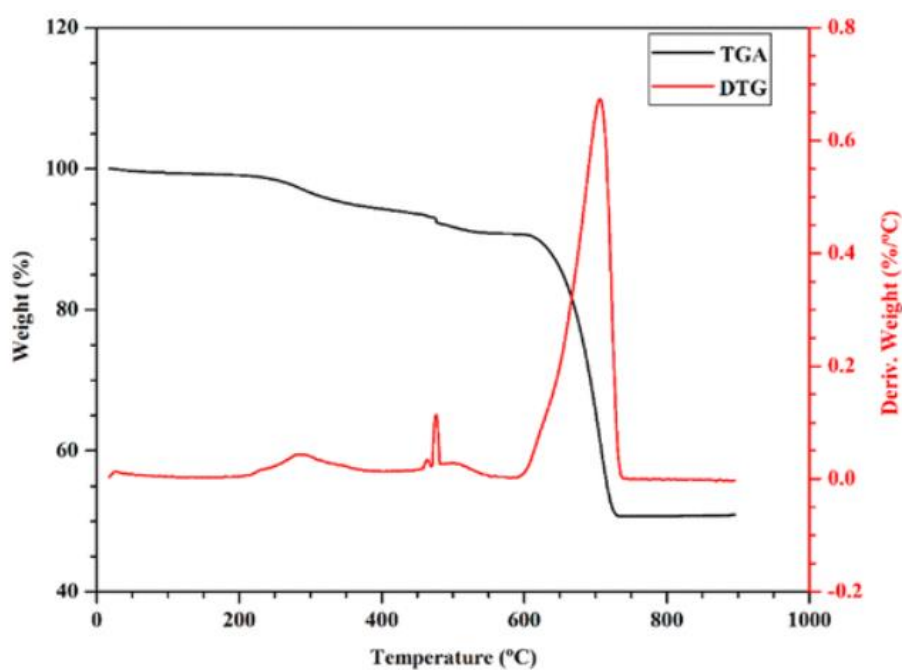


Figure 4.2: TGA Analysis of Chicken Eggshells (Fayyazi, et al., 2018).

Table 4.2: TGA Analysis of Various Biomass-Derived CaO Catalysts.

Biomass	Stage 1 Temperature (°C)	Stage 2 Temperature (°C)	Weight Loss (%)		References
			Stage	Stage	
			1	2	
Chicken Eggshell	200-450	640-740	8.0	37.2	(Fayyazi, et al., 2018)
<i>Malleus malleus</i> Shell	220-380	650-750	5.6	40.0	(Rabia, et al., 2018)
Cockle Shell	200-300	600-700	5.2	43.5	(Mohamed, et al., 2012)
Razor Shell	250-430	650-800	3.3	41.5	(Reddy, et al., 2017)
Shrimp Shell	150-350	700-850	4.0	25.0	(Sun, Sage and Sun, 2017)
Snail Shell	200-400	650-800	3.5	35.5	(Gendy, Deriase and Hamdy, 2014)
<i>Donax deltoides</i> Shell	260-450	650-800	4.0	41.0	(Niju, Vishnupriya and Balajii, 2019)

4.1.4 Fourier Transform Infrared Spectroscopy (FTIR)

Figure 4.3 shows the FTIR spectra of the catalysts that derived from various biomasses such as chicken eggshell, ostrich eggshell, snail shell and so on while Table 4.3 lists down the significant findings obtained from the FTIR spectra.

By comparing the spectrum of each sample, it can be seen that all the samples showed a similar absorption spectrum. For the uncalcined or raw samples, the sharp peaks ranging between 707 cm^{-1} and 713 cm^{-1} represented the in-plane bending of carbonate molecules (CO_3^{2-}) of CaCO_3 , the peak at values ranging between 859 cm^{-1} and 876 cm^{-1} represented the out-of-plane bending of CO_3^{2-} and the sharp peaks ranging between 1394 cm^{-1} and 1476 cm^{-1} had been assigned to the asymmetric stretching of CO_3^{2-} (Engin, Demirtas and Eken, 2006). Next, the absorption band of organic matter was identified at around 2509 cm^{-1} to 2515 cm^{-1} and 1786 cm^{-1} to 1795 cm^{-1} (Bharti, et al., 2020).

After calcination, it was observed that the absorption peaks of the organic matter decreased or either disappeared. Furthermore, the intensity of the peaks corresponding to the CO_3^{2-} also declined or eventually disappeared. According to Awogbemi, Inambao and Onuh (2020), this was due to the decrement in the mass of the functional group joined to the CO_3^{2-} as carbonate was broken down to CaO during calcination process. In addition, it was seen that all the calcined samples showed a strong absorption band at around 3400 cm^{-1} to 3650 cm^{-1} .

According to Margaretha, et al. (2012), this phenomenon could be assigned to the stretching of $-\text{OH}$ group of calcium hydroxide ($\text{Ca}(\text{OH})_2$). The presence of $-\text{OH}$ group might probably due to the interaction of the calcined samples with the moisture in the surrounding air and subsequently formation of $\text{Ca}(\text{OH})_2$. The results of FTIR analysis once again revealed the decomposition of CaCO_3 through calcination process.

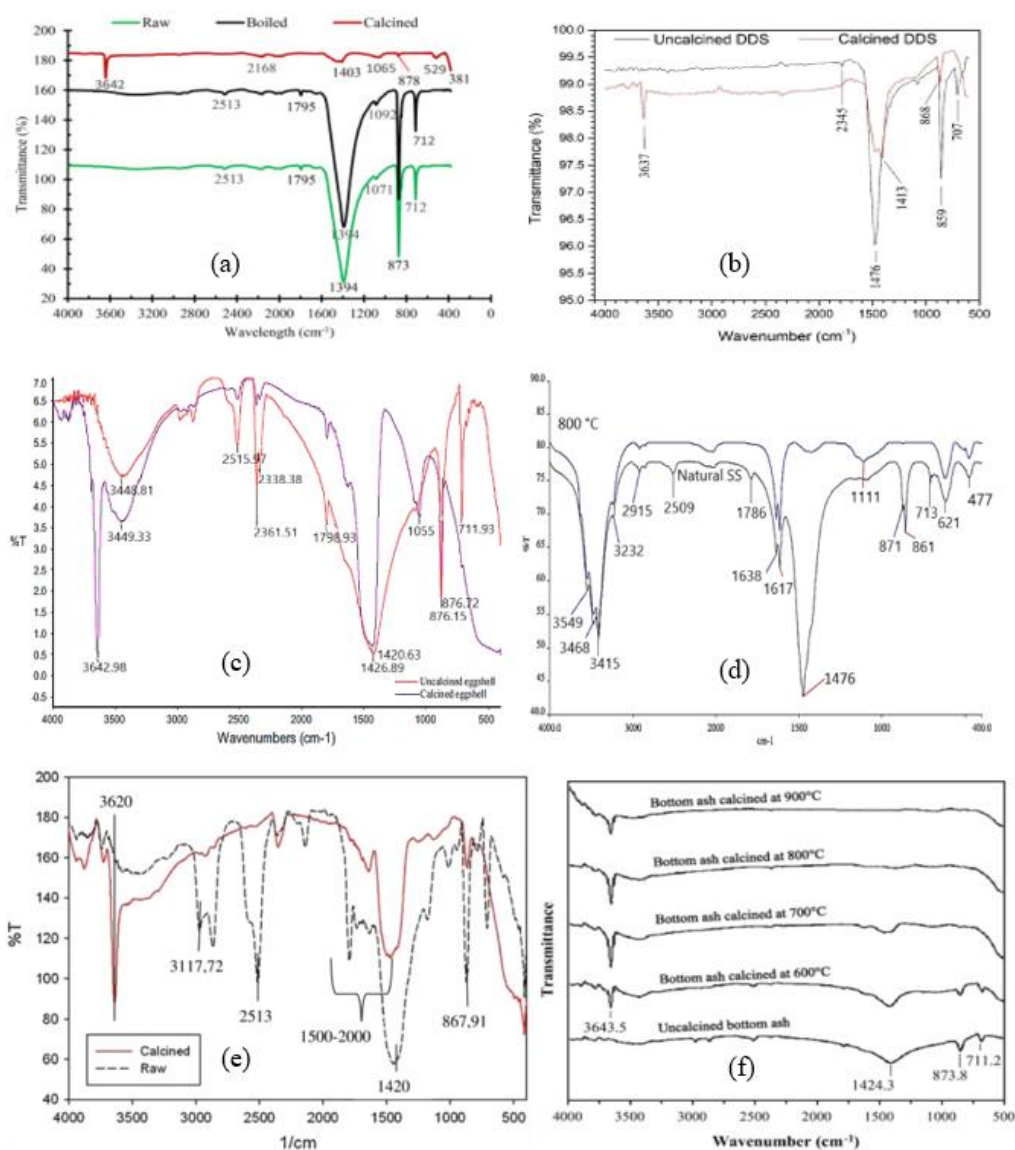


Figure 4.3: FTIR Spectra of (a) Chicken Eggshells Samples (Bharti, et al., 2020), (b) *Donax deltoides* Shells Samples (Niju, Vishnupriya and Balajii, 2019), (c) Ostrich Eggshells Samples (Tan, et al., 2015), (d) Snail Shells Samples (Gendy, Deriase and Hamdy, 2014), (e) *Pomacea* sp. Shells Samples (Margaretha, et al., 2012) and (f) Bottom Ashes Samples (Maneerung, Kawi and Wang, 2015).

Table 4.3: FTIR Analysis of Various Biomass-Derived CaO Catalysts.

Biomass	Wavelength (cm ⁻¹)		Assignment	References
	Raw	Calcined		
Chicken Eggshell	712, 873, 1071, 1394	529, 878, 1065, 1403	bending and stretching of CO ₃ ²⁻	(Bharti, et al., 2020)
	1795, 2513	2168	stretching vibration of organic matter	
	-	3642	stretching vibration of –OH group	
<i>Donax deltoides</i> Shell	707, 859, 1476	868, 1413	bending and stretching of CO ₃ ²⁻	(Niju, Vishnupriya and Balajii, 2019)
	2345	-	stretching vibration of organic matter	
	-	3637	stretching vibration of –OH group	
Ostrich Eggshell	711, 876, 1055, 1420	1055, 1426	bending and stretching of CO ₃ ²⁻	(Tan, et al., 2015)
	1798, 2515	-	stretching vibration of organic matter	
	-	3642	stretching vibration of –OH group	

Table 4.3: (continued)

Biomass	Wavelength (cm ⁻¹)		Assignment	References
	Raw	Calcined		
Snail Shell	713, 861, 871, 1476	-	bending and stretching of CO ₃ ²⁻	(Gendy, Deriase and Hamdy, 2014)
	1786, 2509	-	stretching vibration of organic matter	
	3415	3468, 3549	stretching vibration of –OH group	
<i>Pomacea</i> sp. Shell	867, 1420	1500	bending and stretching of CO ₃ ²⁻	(Margaretha, et al., 2012)
	2513	-	stretching vibration of organic matter	
	-	3620	stretching vibration of –OH group	
Bottom Ash	711, 873, 1424	-	bending and stretching of CO ₃ ²⁻	(Maneerung, Kawi and Wang, 2015)
	-	-	stretching vibration of organic matter	
	-	3643	stretching vibration of –OH group	

4.1.5 X-ray Diffraction (XRD) Analysis

Table 4.4 tabulates the findings obtained from the XRD spectrum of the biomass-derived CaO catalysts while Figure 4.4 depicts the XRD patterns of those CaO catalysts.

It was observed that most of the samples showed similar peaks at around 32° , 37° , 54° , 64° and 67° . According to Bharti, et al. (2020), these peaks were attributed to the presence of CaO in the catalyst samples, which is also in agreement with the XRD pattern of the pure CaO. However, the other peaks at around 18° , 34.0° , 48.0° , 51.0° and 62.0° were observed in the calcined chicken eggshell, calcined ostrich eggshell, calcined *Donax deltoidea* shell and calcined *Pomacea* sp. shell catalysts as shown in Figure 4.4 (a), Figure 4.4 (b) and Figure 4.4 (d). These peaks were ascribed to Ca(OH)_2 and the presence of Ca(OH)_2 in the samples might be due to the exposure of the catalyst to the surrounding air during analysis, leading to the formation of Ca(OH)_2 (Chen, et al., 2014).

Next, Figure 4.4 (e) and Figure 4.4 (f) depict the XRD patterns of the bottom ash samples and snail shell samples at different calcination temperatures. At temperatures below 700°C , a tall peak at around 29° and some small peaks between 30° and 50° were detected, which were attributed to CaCO_3 as reported by Gendy, Deriase and Hamdy (2014).

The absence of CaCO_3 peaks and the presence of CaO peaks at temperatures above 800°C indicated that the CaCO_3 was completely decomposed into CaO, which is in agreement with the result obtained from the TGA analysis as discussed earlier in Section 4.1.3. According to Oliveira, Teleken and Alves (2020), the activity of the catalyst in biodiesel production could be enhanced through the conversion of CaCO_3 to CaO in the calcined catalyst sample.

Table 4.4: XRD Analysis of Various Biomass-Derived CaO Catalysts.

Catalyst Sample	Peaks Corresponding to CaO	Peaks Corresponding to Ca(OH) ₂	References
Calcined Commercial CaO (Pure CaO)	27.5°, 32.5°, 37.5°, 54.5°, 64.5°, 68°	-	(Tan, et al., 2015)
Calcined Chicken Eggshell	27.5°, 54.5°, 64.5°	34°, 48°, 51°, 62°	(Tan, et al., 2015)
Calcined Ostrich Eggshell	27.5°, 32.5°, 37.5°, 54.5°, 64.5°, 68°	34°, 48°, 51°, 62°	(Tan, et al., 2015)
Calcined <i>Donax deltoides</i> Shell	32.2°, 37.4°, 53.9°, 64.2°, 67.4°, 79.7°, 88.6°	18°, 34.2°, 47.2°, 50.9°	(Niju, Vishnupriya and Balajii, 2019)
Calcined <i>Malleus malleus</i> Shell	32.2°, 37.4°, 53.9°, 64.2°, 67.4°, 79.6°, 88.5°	-	(Rabia, et al., 2018)
Calcined <i>Pomacea</i> sp. Shell	32.2°, 37.3°, 53.8°	18°, 28.6°, 34.1°, 47°, 50.8°	(Margaretha, et al., 2012)
Calcined Bottom Ash	32.2°, 37.4°, 53.8°, 65.2°, 67.5°	-	(Maneerung, Kawi and Wang, 2015)
Calcined Snail Shell	32.5°, 37.5°, 54.4°, 64.5°, 68°	-	(Gendy, Deriase and Hamdy, 2014)

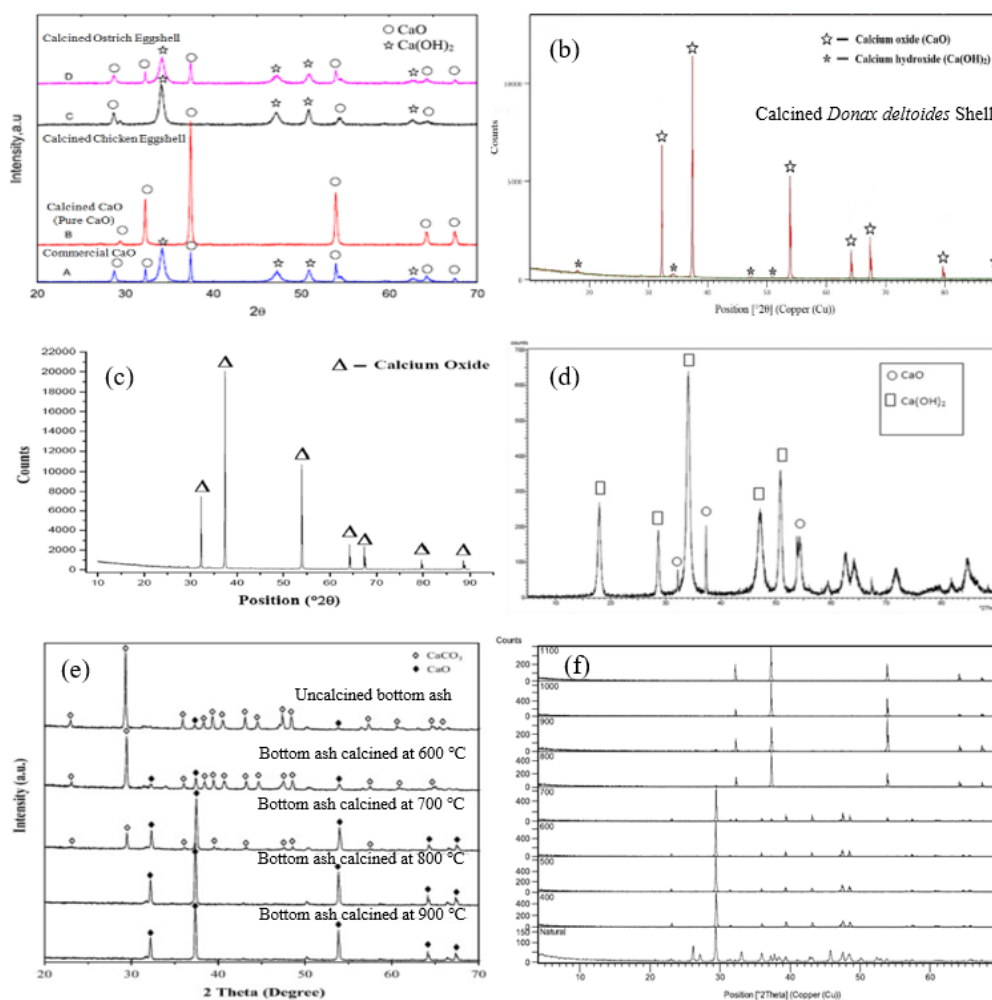


Figure 4.4: XRD Patterns of (a) Commercial CaO, Calcined Commercial CaO (Pure CaO), Calcined Chicken Eggshell and Calcined Ostrich Eggshell (Tan, et al., 2015), (b) Calcined *Donax deltoides* Shell (Niju, Vishnupriya and Balajii, 2019), (c) Calcined *Malleus malleus* Shell (Rabia, et al., 2018), (d) Calcined *Pomacea* sp. Shell (Margaretha, et al., 2012), (e) Calcined Bottom Ash (Maneerung, Kawi and Wang, 2015) and (f) Calcined Snail Shell (Gendy, Deriase and Hamdy, 2014).

4.2 Design Expert Simulation

4.2.1 Development of Regression Model and Model Accuracy Check

CCD combined with response surface modelling was applied to study the influence of various process variables on the biodiesel yield. Tables 4.5 to 4.9 show the results obtained for different types of biomass-derived CaO catalysts at the process conditions set by the CCD.

Table 4.5: Experiment Matrix and Response for CaO Catalyst Derived from Chicken Eggshell.

Run	A: Methanol to Oil Ratio	B: Catalyst Concentration (wt. %)	C: Reaction Time (h)	D: Reaction Temperature (°C)	Biodiesel Yield (%)
1	10:1	1.5	1.5	65	91.00
2	12:1	2	1	50	80.50
3	8:1	2	1	80	90.50
4	10:1	1.5	1.5	65	90.50
5	10:1	1.5	1.5	65	91.50
6	14:1	1.5	1.5	65	94.00
7	10:1	1.5	0.5	65	74.00
8	8:1	1	2	50	84.20
9	10:1	1.5	1.5	35	72.50
10	8:1	1	1	80	84.40
11	8:1	2	2	80	91.00
12	12:1	1	1	80	89.90
13	12:1	2	2	80	94.10
14	8:1	2	2	50	85.50

Table 4.5: (continued)

Run	A: Methanol to Oil Ratio	B: Catalyst Concentration (wt. %)	C: Reaction Time (h)	D: Reaction Temperature (°C)	Biodiesel Yield (%)
15	12:1	1	1	50	71.20
16	6:1	1.5	1.5	65	81.80
17	8:1	2	1	50	74.00
18	12:1	1	2	50	90.00
19	10:1	0.5	1.5	65	83.10
20	10:1	2.5	1.5	65	91.80
21	10:1	1.5	1.5	95	94.50
22	10:1	1.5	1.5	65	91.00
23	10:1	1.5	2.5	65	92.90
24	8:1	1	2	80	90.50
25	12:1	1	2	80	94.00
26	8:1	1	1	50	65.20
27	10:1	1.5	1.5	65	90.50
28	10:1	1.5	1.5	65	90.00
29	12:1	2	1	80	94.00
30	12:1	2	2	50	90.90

Table 4.6: Experiment Matrix and Response for CaO Catalyst Derived from Ostrich Eggshell.

Run	A: Methanol to Oil Ratio	B: Catalyst Concentration (wt. %)	C: Reaction Time (h)	D: Reaction Temperature (°C)	Biodiesel Yield (%)
1	12:1	2	2	50	89.30
2	10:1	1.5	1.5	65	96.50
3	8:1	1	1	50	65.70
4	10:1	1.5	1.5	35	71.00
5	12:1	1	1	50	70.80
6	8:1	2	1	80	87.30
7	10:1	1.5	1.5	65	95.60
8	8:1	1	2	50	84.90
9	10:1	0.5	1.5	65	88.20
10	12:1	2	2	80	92.80
11	12:1	1	1	80	85.70
12	12:1	1	2	50	88.00
13	10:1	2.5	1.5	65	93.10
14	10:1	1.5	1.5	95	90.30

Table 4.6: (continued)

Run	A: Methanol to Oil Ratio	B: Catalyst Concentration (wt. %)	C: Reaction Time (h)	D: Reaction Temperature (°C)	Biodiesel Yield (%)
15	10:1	1.5	0.5	65	66.70
16	12:1	1	2	80	90.30
17	8:1	2	1	50	66.10
18	8:1	1	1	80	80.80
19	10:1	1.5	1.5	65	95.60
20	14:1	1.5	1.5	65	89.10
21	10:1	1.5	1.5	65	95.60
22	8:1	2	2	50	80.70
23	8:1	1	2	80	84.70
24	10:1	1.5	2.5	65	89.20
25	10:1	1.5	1.5	65	97.30
26	6:1	1.5	1.5	65	75.70
27	12:1	2	1	80	95.80
28	12:1	2	1	50	78.60
29	8:1	2	2	80	86.00
30	10:1	1.5	1.5	65	95.60

Table 4.7: Experiment Matrix and Response for CaO Catalyst Derived from Snail Shell.

Run	A: Methanol to Oil Ratio	B: Catalyst Concentration (wt. %)	C: Reaction Time (h)	Biodiesel Yield (%)
1	9:1	6	3	80.80
2	7.5:1	6	2	85.00
3	7.5:1	9	2	92.50
4	7.5:1	9	1	89.20
5	7.5:1	9	2	92.22
6	6:1	12	1	83.40
7	7.5:1	9	2	92.25
8	7.5:1	9	2	92.48
9	6:1	6	1	89.80
10	7.5:1	9	2	92.40
11	7.5:1	9	2	92.00
12	6:1	12	3	74.40
13	9:1	6	1	71.40
14	7.5:1	9	2	92.60
15	9:1	12	1	68.00
16	7.5:1	9	2	92.31
17	6:1	9	2	90.60
18	7.5:1	12	2	84.00
19	7.5:1	9	3	87.00
20	9:1	9	2	87.40

Table 4.8: Experiment Matrix and Response for CaO Catalyst Derived from *Donax deltoides* Shell.

Run	A: Methanol to Oil Ratio (% v/v)	B: Catalyst Concentration (wt. %)	C: Reaction Time (min)	Biodiesel Yield (%)
1	72	8	99.55	83.00
2	72	4.64	150	38.80
3	72	8	150	76.70
4	82	6	180	67.00
5	72	8	150	76.70
6	62	6	120	91.60
7	72	8	200.45	65.00
8	62	6	180	48.20
9	55.18	8	150	95.10
10	72	8	150	76.20
11	72	8	150	75.80
12	72	11.36	150	29.10
13	72	8	150	76.80
14	72	8	150	76.70
15	82	6	120	49.10
16	62	10	180	48.20
17	62	10	120	95.00
18	82	10	120	23.90
19	82	10	180	59.10
20	88.82	8	150	57.70

Table 4.9: Experiment Matrix and Response for CaO Catalyst Derived from *Malleus malleus* Shell.

Run	A: Methanol to Oil Ratio	B: Catalyst Concentration (wt. %)	C: Reaction Time (min)	Biodiesel Yield (%)
1	12:1	2	60	30.00
2	15:1	1.5	90	52.00
3	6:1	2	60	44.00
4	6:1	1	120	75.00
5	3:1	1.5	90	44.00
6	12:1	1	60	86.00
7	12:1	1	120	70.00
8	12:1	2	120	97.00
9	9:1	1.5	90	55.00
10	6:1	2	120	92.00
11	9:1	1.5	90	78.00
12	9:1	2.5	90	91.00
13	9:1	1.5	30	60.00
14	9:1	1.5	90	95.00
15	6:1	1	60	90.00
16	9:1	0.5	90	88.00
17	9:1	1.5	90	91.00
18	9:1	1.5	150	90.00
19	9:1	1.5	90	89.00
20	9:1	1.5	90	91.00

A second-order quadratic model was suggested by the software to predict the optimum operating conditions of the biodiesel production for all the developed models. The results of the ANOVA for each model were presented in Tables 4.10 to 4.14.

Table 4.10: ANOVA and Fit Statistics Results for Chicken Eggshell-Derived CaO Catalyst Model.

Source	Sum of Squares	df	Mean Square	F-value	p-value	Characteristics
Model	1833.34	14	130.95	262.40	< 0.0001	Significant
A	169.07	1	169.07	338.78	< 0.0001	Significant
B	98.01	1	98.01	196.39	< 0.0001	Significant
C	488.70	1	488.70	979.26	< 0.0001	Significant
D	713.95	1	713.95	1430.60	< 0.0001	Significant
AB	0.3306	1	0.3306	0.6625	0.4284	Not significant
AC	0.8556	1	0.8556	1.71	0.2101	Not significant
AD	4.10	1	4.10	8.22	0.0118	Significant
BC	40.64	1	40.64	81.44	< 0.0001	Significant
BD	5.64	1	5.64	11.30	0.0043	Significant
CD	149.45	1	149.45	299.47	< 0.0001	Significant
A²	13.64	1	13.64	27.33	0.0001	Significant
B²	18.34	1	18.34	36.75	< 0.0001	Significant
C²	90.63	1	90.63	181.59	< 0.0001	Significant
D²	89.38	1	89.38	179.11	< 0.0001	Significant
Residual	7.49	15	0.4991			
Fit Statistics						
	R²				0.9959	
	Predicted R²				0.9921	
	Adjusted R²				0.9798	
	Adequate Precision				60.0985	
	Standard Deviation				0.7064	
	Mean				86.63	

Table 4.11: ANOVA and Fit Statistics Results for Ostrich Eggshell-Derived CaO Catalyst Model.

Source	Sum of Squares	df	Mean Square	F-value	p-value	Characteristics
Model	2704.93	14	193.21	128.48	< 0.0001	Significant
A	279.48	1	279.48	185.85	< 0.0001	Significant
B	52.51	1	52.51	34.92	< 0.0001	Significant
C	512.45	1	512.45	340.76	< 0.0001	Significant
D	579.18	1	579.18	385.14	< 0.0001	Significant
AB	19.58	1	19.58	13.02	0.0026	Significant
AC	2.98	1	2.98	1.98	0.1799	Not significant
AD	0.7656	1	0.7656	0.5091	0.4856	Not significant
BC	35.70	1	35.70	23.74	0.0002	Significant
BD	14.25	1	14.25	9.48	0.0076	Significant
CD	206.64	1	206.64	137.41	< 0.0001	Significant
A²	316.88	1	316.88	210.71	< 0.0001	Significant
B²	48.99	1	48.99	32.58	< 0.0001	Significant
C²	558.26	1	558.26	371.23	< 0.0001	Significant
D²	403.71	1	403.71	268.45	< 0.0001	Significant
Residual	22.56	15	1.50			
Fit Statistics						
	R²				0.9917	
	Predicted R²				0.9840	
	Adjusted R²				0.9564	
	Adequate Precision				35.9759	
	Standard Deviation				1.23	
	Mean				85.57	

Table 4.12: ANOVA and Fit Statistics Results for Snail Shell-Derived CaO Catalyst Model.

Source	Sum of Squares	df	Mean Square	F-value	p-value	Characteristics
Model	1240.65	9	137.85	182.18	< 0.0001	Significant
A	84.10	1	84.10	111.15	< 0.0001	Significant
B	24.34	1	24.34	32.16	< 0.0001	Significant
C	0.1440	1	0.1440	0.1903	0.6693	Not significant
AB	4.81	1	4.81	6.35	0.0245	Significant
AC	218.41	1	218.41	288.65	< 0.0001	Significant
BC	3.13	1	3.13	4.13	0.0616	Not significant
A²	23.00	1	23.00	30.39	< 0.0001	Significant
B²	151.69	1	151.69	200.48	< 0.0001	Significant
C²	39.69	1	39.69	52.45	< 0.0001	Significant
Residual	10.59	10	0.7566			
Fit Statistics						
	R²				0.9915	
	Predicted R²				0.9861	
	Adjusted R²				0.9396	
	Adequate Precision				41.7709	
	Standard Deviation				0.8699	
	Mean				86.36	

Table 4.13: ANOVA and Fit Statistics Results for *Donax deltoides* Shell-Derived CaO Catalyst Model.

Source	Sum of Squares	df	Mean Square	F-value	p-value	Characteristics
Model	8138.83	9	904.31	151.02	< 0.0001	Significant
A	1577.96	1	1577.96	263.53	< 0.0001	Significant
B	155.03	1	155.03	25.89	0.0005	Significant
C	332.36	1	332.36	55.51	< 0.0001	Significant
AB	166.53	1	166.53	27.81	0.0004	Significant
AC	2566.86	1	2566.86	428.68	< 0.0001	Significant
BC	24.15	1	24.15	4.03	0.0724	Not significant
A²	0.1106	1	0.1106	0.0185	0.8946	Not significant
B²	3284.16	1	3284.16	548.47	< 0.0001	Significant
C²	12.63	1	12.63	2.11	0.1771	Not significant
Residual	59.88	10	5.99			
Fit Statistics						
	R²				0.9927	
	Predicted R²				0.9861	
	Adjusted R²				0.9348	
	Adequate Precision				39.0319	
	Standard Deviation				2.45	
	Mean				65.48	

Table 4.14: ANOVA and Fit Statistics Results for *Malleus malleus* Shell-Derived CaO Catalyst Model.

Source	Sum of Squares	df	Mean Square	F-value	p-value	Characteristics
Model	6474.05	9	719.34	4.69	0.0121	Significant
A	0.25	1	0.25	0.0016	0.9686	Not significant
B	169.00	1	169.00	1.10	0.3187	Not significant
C	1296.00	1	1296.00	8.44	0.0157	Significant
AB	0.0000	1	0.0000	0.0000	1.0000	Not significant
AC	40.50	1	40.50	0.2639	0.6186	Not significant
BC	2664.50	1	2664.50	17.36	0.0019	Significant
A²	1980.39	1	1980.39	12.90	0.0049	Significant
B²	56.57	1	56.57	0.3686	0.5573	Not significant
C²	113.54	1	113.54	0.7398	0.4099	Not significant
Residual	1534.75	10	153.48			
Fit Statistics						
	R²				0.8084	
	Predicted R²				0.6359	
	Adjusted R²				0.3746	
	Adequate Precision				6.7352	
	Standard Deviation				12.39	
	Mean				75.40	

Based on the results shown in Tables 4.10 to 4.14, the *F*-value for the chicken eggshell model was 262.40, the *F*-value for the ostrich eggshell model was 128.48, while the *F*-values for the snail shell model, *Donax deltoides* shell model and *Malleus malleus* shell model were found to be 182.18, 151.02 and 4.69, respectively. For all developed models, the *p*-values were shown to be less than 0.05, verifying that the developed models were statistically significant.

In addition, the process parameters that generate appreciable effects on the biodiesel yield for each model can be observed from the results of ANOVA. By taking the chicken eggshell model as an example, the methanol

to oil ratio, catalyst concentration, reaction time and reaction temperature terms (A, B, C and D), as well as their interaction terms and squared terms shown by AD, BC, BD, CD, A², B², C² and D² were considered as significant model terms as their *p*-values were less than 0.05. AB and AC were not significant as the *p*-values were greater than 0.1. By excluding the trivial process parameters (insignificant terms), the following equations that correlate the biodiesel yield to the process parameters for each model in terms of coded factors were acquired.

The chicken eggshell model:

$$\begin{aligned} \text{Biodiesel Yield (\%)} = & 90.75 + 2.65A + 2.02B + 4.51C + 5.45D - \\ & 0.5062AD - 1.59BC - 0.5937BD - 3.06CD - 0.7052A^2 - \\ & 0.8177B^2 - 1.82C^2 - 1.81D^2 \end{aligned} \quad (4.1)$$

The ostrich eggshell model:

$$\begin{aligned} \text{Biodiesel Yield (\%)} = & 96.03 + 3.41A + 1.48B + 4.62C + 4.91D + \\ & 1.11AB - 1.49BC + 0.9438BD - 3.59CD - 3.40A^2 - 1.34B^2 - \\ & 4.51C^2 - 3.84D^2 \end{aligned} \quad (4.2)$$

The snail shell model:

$$\begin{aligned} \text{Biodiesel Yield (\%)} = & 92.20 - 2.90A - 1.56B + 0.7750AB + \\ & 5.23AC - 2.87A^2 - 7.37B^2 - 3.77C^2 \end{aligned} \quad (4.3)$$

The *Donax deltoides* shell model:

$$\begin{aligned} \text{Biodiesel Yield (\%)} = & 76.49 - 10.75A - 3.37B - 4.93C - 4.56AB + \\ & 17.91AC - 15.10B^2 \end{aligned} \quad (4.4)$$

The *Malleus malleus* shell model:

$$\text{Biodiesel Yield (\%)} = 83.00 + 9.00C + 18.25BC - 8.88A^2 \quad (4.5)$$

where

A = methanol to oil ratio

B = catalyst concentration

C = reaction time

D = reaction temperature

According to Tan, et al. (2017), model with large coefficient of determination or R^2 values can have high level of multicollinearity to support the model and an R^2 value of at least 0.8 indicates a good fitness of the data for the model. It was observed that the R^2 values in Tables 4.10 to 4.14 were greater than 0.8 ($R^2 = 0.9959$ for chicken eggshell model, $R^2 = 0.9917$ for ostrich eggshell model, $R^2 = 0.9915$ for snail shell model, $R^2 = 0.9927$ for *Donax deltoides* shell model and $R^2 = 0.8084$ for *Malleus malleus* shell model), which were also close to the unity, indicating that the developed models can accurately explained the relationship between the biodiesel yield and the process parameters. Moreover, the adequate precision values for the chicken eggshell model, ostrich eggshell model, snail shell model, *Donax deltoides* shell model and *Malleus malleus* shell model were 60.0985, 35.9759, 41.7709, 39.0319 and 6.7352, respectively, which were greater than 4. This shows that the developed models have adequate signals for the optimisation to be performed.

Next, Figure 4.5 shows the normal plot of residuals for the developed models where the normal probability is plotted against the externally studentised residuals. It was notable that the points were plotted approximately along the straight line, showing that the transformation of response is not required for the models as the results meet the criteria of normality.

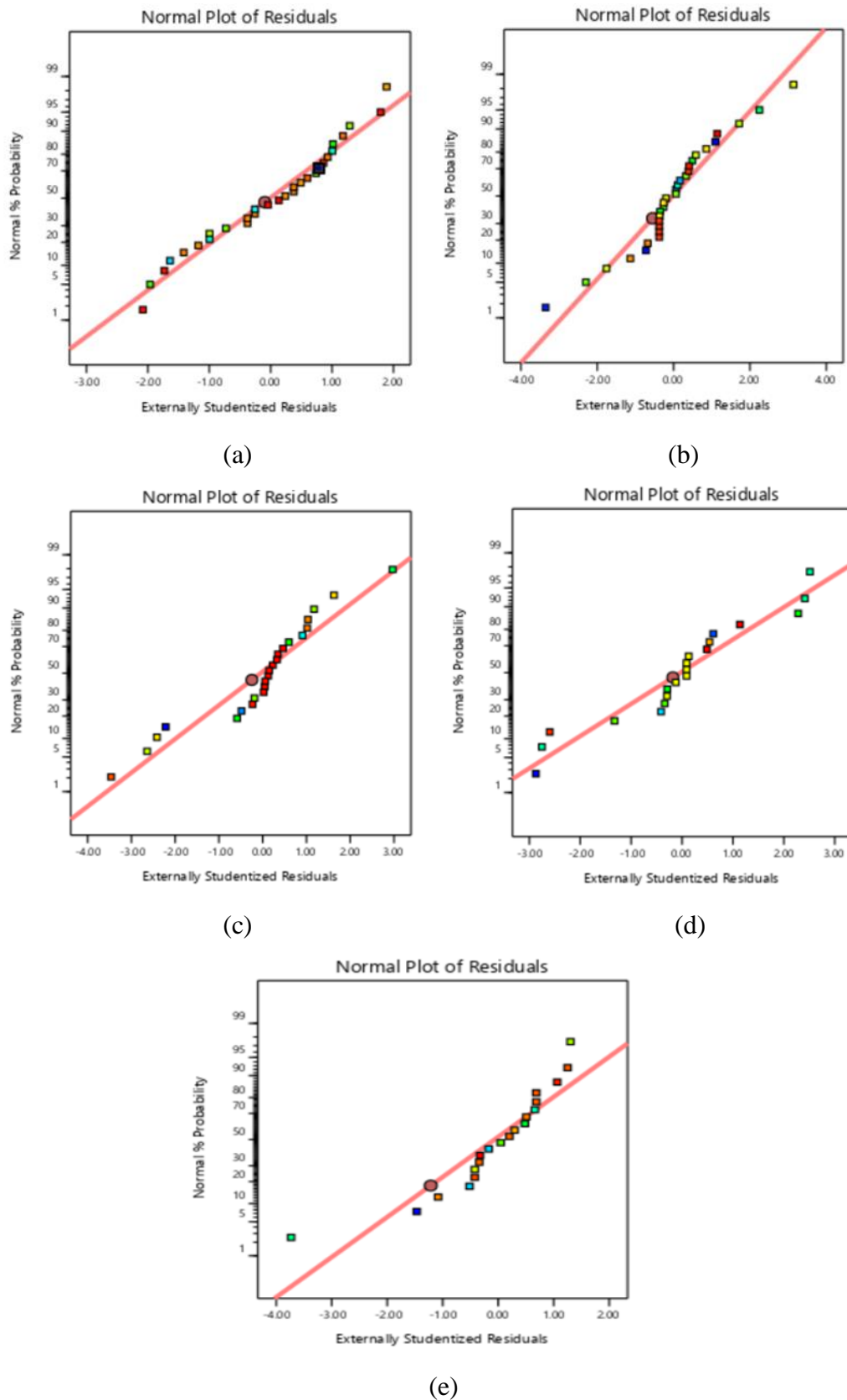


Figure 4.5: Normal Plot of Residuals for the (a) Chicken Eggshell Model, (b) Ostrich Eggshell Model, (c) Snail Shell Model, (d) *Donax deltoides* Shell Model and (e) *Malleus malleus* Shell Model.

4.2.2 Interaction between Parameters

RSM was applied to investigate the interaction relationship between the process parameters affecting the biodiesel yield. The interaction between methanol to oil ratio (A), catalyst concentration (B), reaction time (C) and reaction temperature (D) was studied in the chicken eggshell model and ostrich eggshell model. On the other hand, the interaction between methanol to oil ratio (A), catalyst concentration (B) and reaction time (C) was studied in the snail shell model, *Donax deltoideis* shell model and *Malleus malleus* shell model. Only the interaction term that was considered as significant model term will affect the biodiesel yield significantly.

4.2.2 (a) Interaction between Methanol to Oil Ratio (A) and Catalyst Concentration (B)

Based on Tables 4.10 to 4.14, the term AB was significant in ostrich eggshell model, snail shell model and *Donax deltoideis* shell model. Figure 4.6 shows the three-dimensional response surface plots for the interaction between methanol to oil ratio and catalyst concentration while keeping other parameters at a constant value. For the ostrich eggshell model, it was observed from Figure 4.6 (a) that raising the methanol to oil ratio from 8:1 to 11:1 and catalyst concentration from 1 wt. % to 1.9 wt. % increased the biodiesel yield to a maximum value of around 97 %. This was because high methanol to oil ratio might lead to a mass transfer problem, therefore, more catalyst loading was needed to accomplish the complete conversion (Gupta and Rathod, 2019). Furthermore, the biodiesel yield showed an increasing trend at any point of the methanol to oil ratio when the catalyst loading increasing to some extent. This could be supported by the fact that increasing the catalyst concentration meant that there was more number of active sites available to catalyse the reaction (Ramli and Farooq, 2015).

A similar observation was obtained in the snail shell model which showed the highest biodiesel yield of around 92 % was recorded when the methanol to oil ratio and the catalyst loading increased to 7.5:1 and 9 wt. % respectively as shown in Figure 4.6 (b). For the *Donax deltoideis* shell model as shown in Figure 4.6 (c), increasing the catalyst concentration from 6 wt. % to

8 wt. % would increase the biodiesel yield, while increasing the methanol to oil volumetric ratio beyond 62 % reduced the biodiesel yield.

It was also observed that further increment of catalyst loading and methanol to oil ratio beyond those points in each model caused a decline in the biodiesel yield. This was due to the poor diffusion among the oil, methanol and solid catalyst phases when an excess amount of catalyst was used and therefore reducing the biodiesel yield (Rashid, et al., 2011). According to Narowska, Kulazynski and Lukaszewicz (2020), excessive amount of catalyst might also lead to soap formation which would interrupt the transesterification process. Next, the solubility of the glycerol in the product phase increased in excess methanol condition and this resulted in difficulty in separation of FAME, causing a drop in the biodiesel yield (Niju, Vishnupriya and Balajii, 2019).

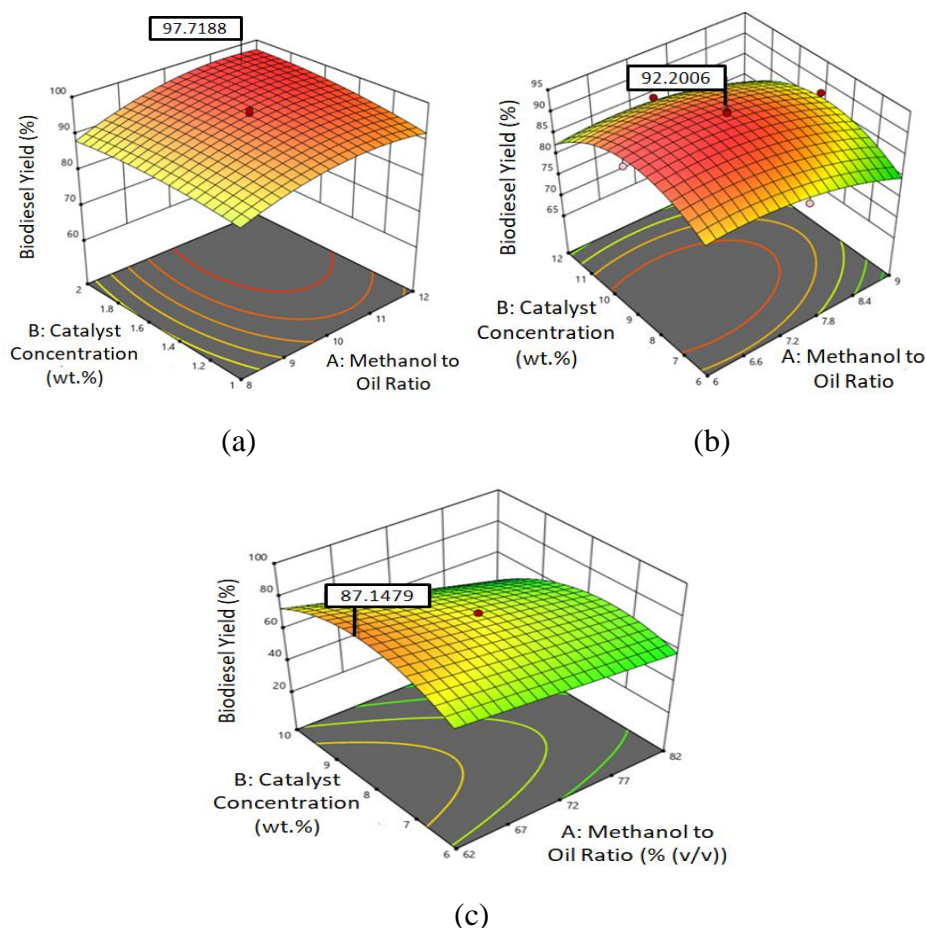
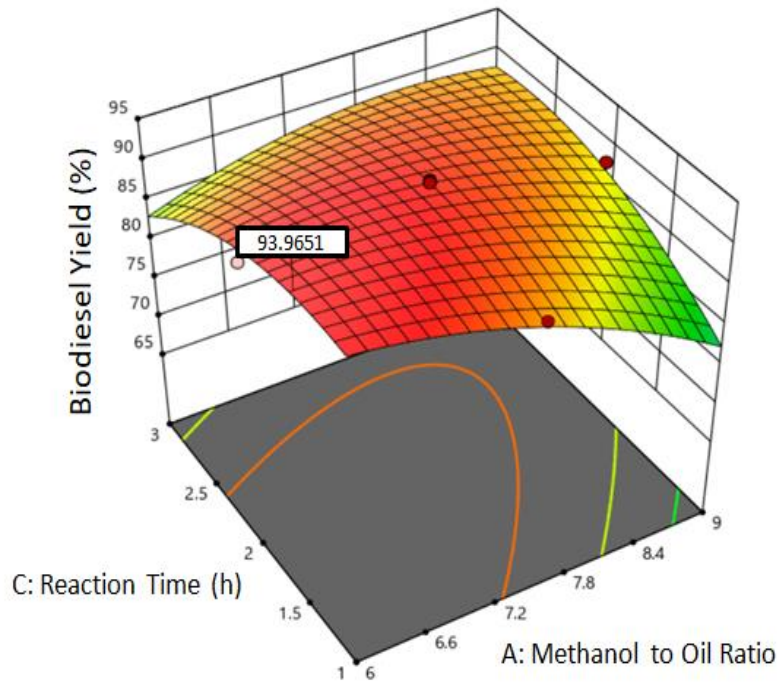


Figure 4.6: Interaction Effect between Methanol to Oil Ratio and Catalyst Concentration on Biodiesel Yield for the (a) Ostrich Eggshell Model, (b) Snail Shell Model and (c) *Donax deltoides* Shell Model.

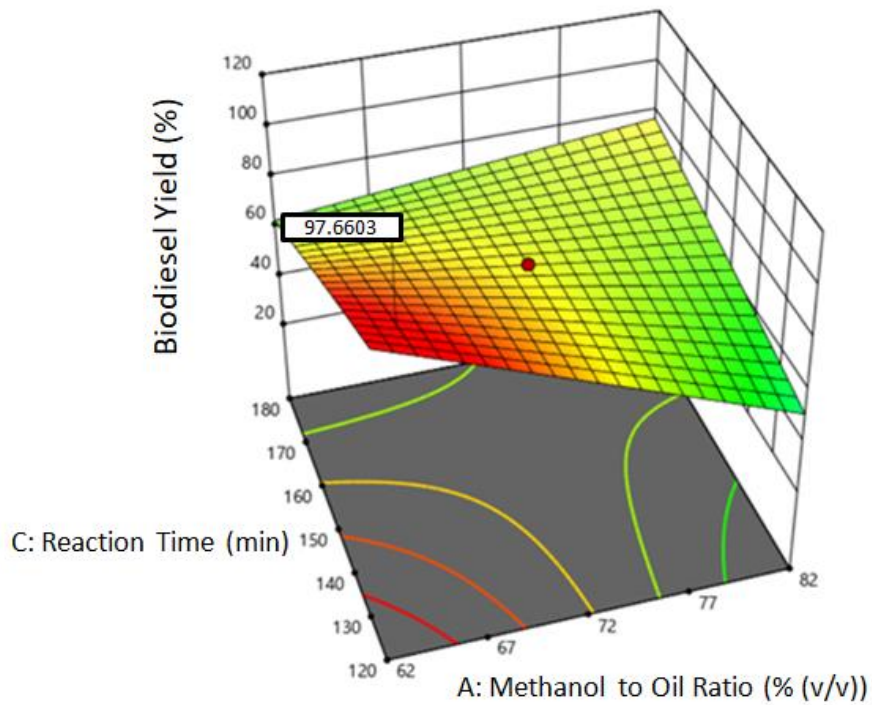
4.2.2 (b) Interaction between Methanol to Oil Ratio (A) and Reaction Time (C)

The term AC was significant in snail shell model and *Donax deltoids* shell model. Figure 4.7 represents the interaction effect between methanol to oil ratio and reaction time on biodiesel yield. A maximum biodiesel yield was observed at a low level of methanol to oil ratio and reaction time for both models. At 6:1 methanol to oil ratio and 1.5 hours reaction time, the highest biodiesel yield of the snail shell model was obtained which was around 94 % as shown in Figure 4.7 (a). For *Donax deltoids* shell model, the maximum biodiesel yield of 97.66 % was found at a reaction time of 130 minutes and methanol to oil volumetric ratio within the range of 62 % to 67 % as shown in Figure 4.7 (b). Then, the biodiesel yield declined when the methanol to oil ratio and reaction time continued to increase.

Methanol acts as a reactant or substrate in the transesterification reaction. High amount of substrate would shift the equilibrium to right side which favoured the forward reaction (Shuit, et al., 2012). As a result, biodiesel yield increased. However, the biodiesel yield would decline when the methanol to oil ratio was higher than the requirement. For both models, the biodiesel yield showed a decreasing trend when the methanol to oil ratio increased beyond the optimum point. This clearly implied that the use of an excess amount of methanol would create a negative impact on the biodiesel yield as excess methanol could lead to the formation of emulsion, making the separation of FAME became difficult (Dhmees, Rashad and Abdullah, 2019). At fixed methanol to oil ratio, the plots showed that the biodiesel yield increased with an increase in reaction time until the reaction time reached a certain value. Further increment of reaction time caused a decline in the biodiesel yield. This was because more biodiesel would be produced when time passed through. However, according to Shohaimi, and Marodzi (2018), further extension of the reaction time when the chemical equilibrium was reached caused the reaction to shift backward which there would be ester loss and thus declined the biodiesel yield.



(a)



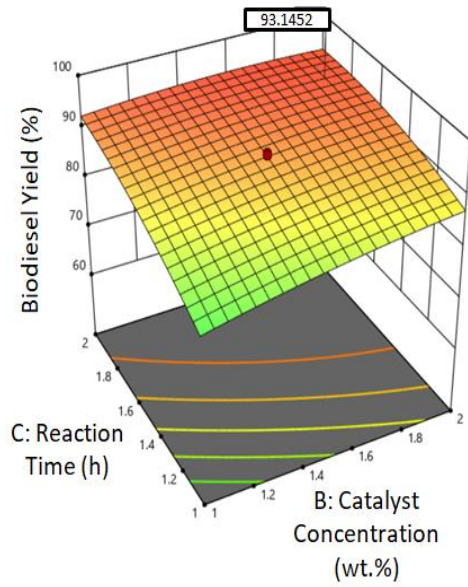
(b)

Figure 4.7: Interaction Effect between Methanol to Oil Ratio and Reaction Time on Biodiesel Yield for the (a) Snail Shell Model and (b) *Donax deltoides* Shell Model.

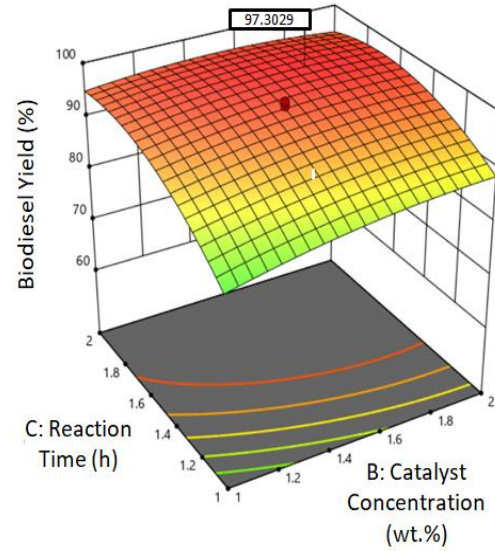
4.2.2 (c) Interaction between Catalyst Concentration (B) and Reaction Time (C)

From the results of ANOVA shown in Tables 4.10 to 4.14, the interactive term BC was significant in the chicken eggshell model, ostrich eggshell model and *Malleus malleus* shell model. Figure 4.8 shows the response surface plots for the interaction between catalyst concentration and reaction time for each model. It was observed from Figure 4.8 (a) and Figure 4.8 (b) that increasing the catalyst concentration and reaction time increased the biodiesel yield in the chicken eggshell model and ostrich eggshell model. A maximum biodiesel yield of 93 % was achieved at a catalyst concentration of 1.9 wt. % and reaction time of 1.8 hours for the chicken eggshell model while the maximum biodiesel yield of 97 % was achieved for the ostrich eggshell model at a catalyst concentration around 1.7 wt. % and 1.7 hours reaction time. According to Santya, Maheswaran and Yee (2019), sufficient supply of catalyst could promote the interaction between the alcohol and the feedstock to yield biodiesel.

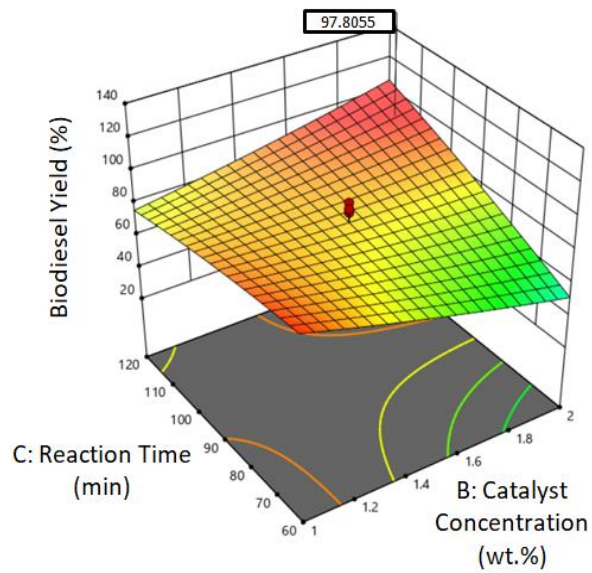
For the *Malleus malleus* shell model shown in Figure 4.8 (c), it was seen that the biodiesel yield dropped with increasing catalyst loading at a fixed low reaction time. The decrement observed with the rise in catalyst loading was probably due to the saponification effect through the use of excessive amount of catalyst (Dhmees, Rashad and Abdullah, 2019). However, the biodiesel yield increased with increasing catalyst concentration at longer reaction time around 100 minutes to 120 minutes. The decrement of biodiesel yield at lower reaction time might be due to the occurrence of incomplete reaction at insufficient reaction time, leading to low biodiesel yield (Santya, Maheswaran and Yee, 2019).



(a)



(b)



(c)

Figure 4.8: Interaction Effect between Catalyst Concentration and Reaction Time on Biodiesel Yield for the (a) Chicken Eggshell Model, (b) Ostrich Eggshell Model and (c) *Malleus malleus* Shell Model.

4.2.2 (d) Interaction between Methanol to Oil Ratio (A) and Reaction Temperature (D)

Among the chicken eggshell model and ostrich eggshell model, the interactive term AD in the chicken eggshell model was significant. From Figure 4.9, the three-dimensional response surface plot shows that raising the methanol to oil ratio from 8:1 to 12:1 and reaction temperature from 50 °C to 80 °C increased the biodiesel yield to a maximum value of around 95.8 %. In this case, the collision theory can be applied for the explanation. At high methanol to oil ratio, there would be more reactant molecules and the kinetic energies of the molecules would increase at high temperatures (Tan, et al., 2017). Then, the reactants molecules would collide more frequently and speed up the rate of reaction. As a result, more biodiesel could be produced at a given reaction time.

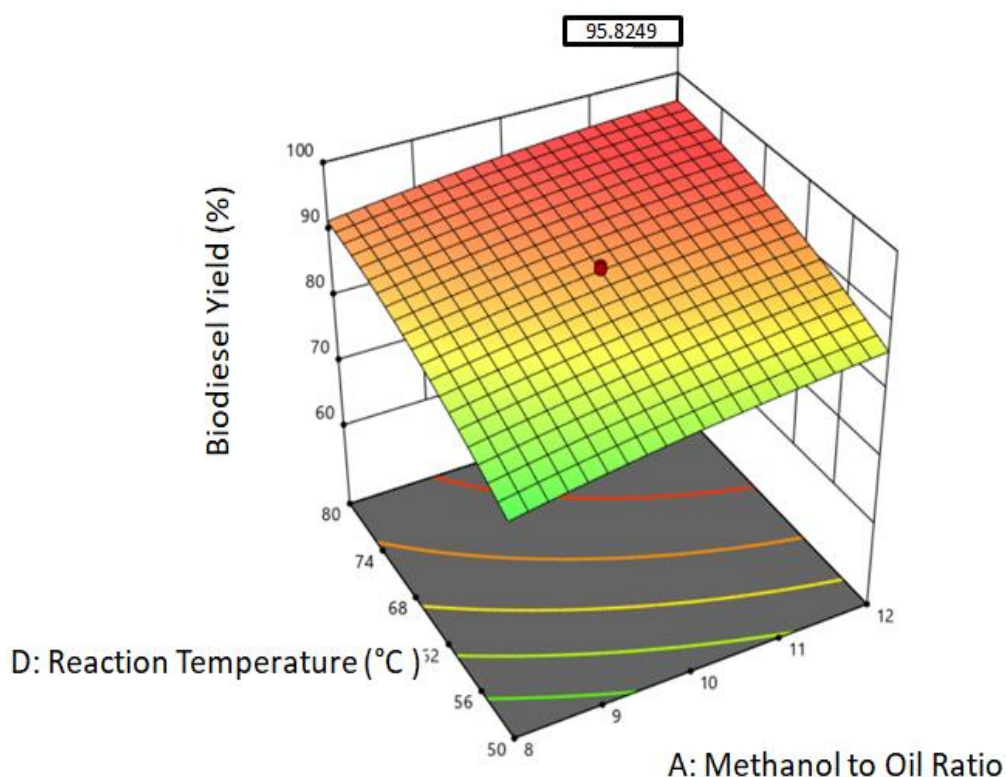
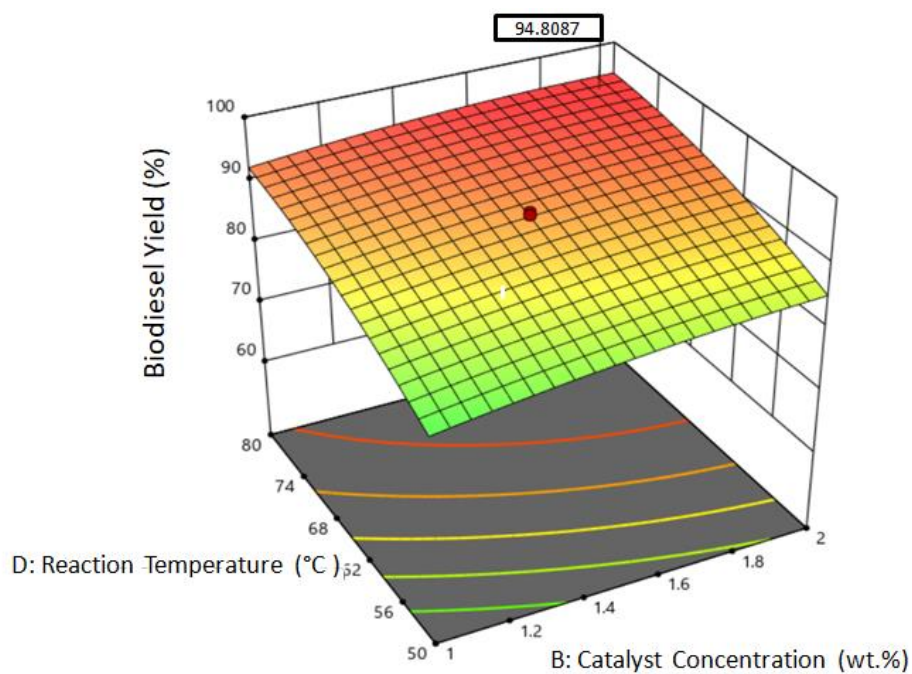


Figure 4.9: Interaction Effect between Methanol to Oil Ratio and Reaction Temperature on Biodiesel Yield for the Chicken Eggshell Model.

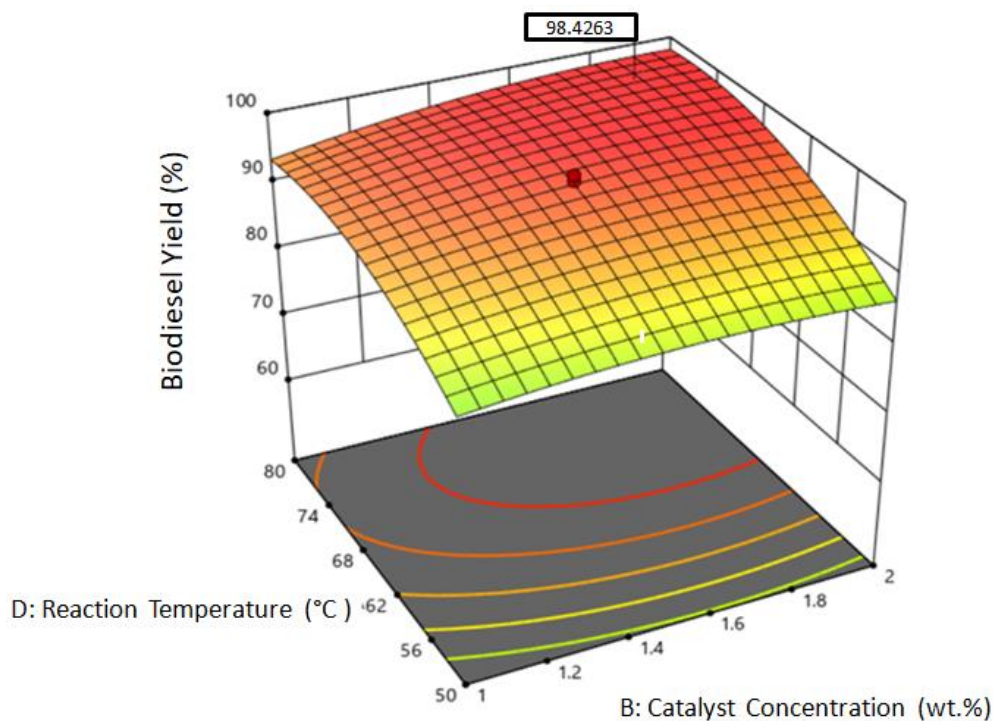
4.2.2 (e) Interaction between Catalyst Concentration (B) and Reaction Temperature (D)

The interactive term BD was significant in both chicken eggshell model and ostrich eggshell model. This meant that the combined effect of catalyst concentration and reaction temperature strongly influenced the biodiesel yield. The plots in Figure 4.10 (a) and Figure 4.10 (b) depict that an increase in catalyst concentration and reaction temperature in both of the models had positive effects on the biodiesel yield. This was because there would be sufficient active sites for the binding of the reactants at high catalyst loading to achieve the maximum biodiesel yield (Al-Muhtaseb, et al., 2018). However, it should be noted that the increment of catalyst concentration beyond the optimum concentration would decline the biodiesel because excess catalyst would lead to a mass transfer limitation as mentioned in the previous section.

Next, transesterification reaction is favored at high temperature as it is an endothermic reaction. According to Tan, et al. (2017), the miscibility of the reactants could be enhanced by increasing the reaction temperature and the reactant molecules would also gain enough energy to pass through the energy barrier. As the catalysts could lower the activation energy, hence the combination of high catalyst loading and high temperature could promote high biodiesel yield as more reactant molecules would have sufficient energy to traverse the smaller energy barrier. Furthermore, it can be seen from Figure 4.10 that the maximum biodiesel yield for both models was observed at reaction temperature between 74 °C to 80 °C. Further increment of temperature caused a drop in the biodiesel yield. This might probably due to the formation of bubble molecules at high temperatures attributed to the excess vaporisation of methanol, which interrupting the reaction (Al-Muhtaseb, et al., 2018).



(a)



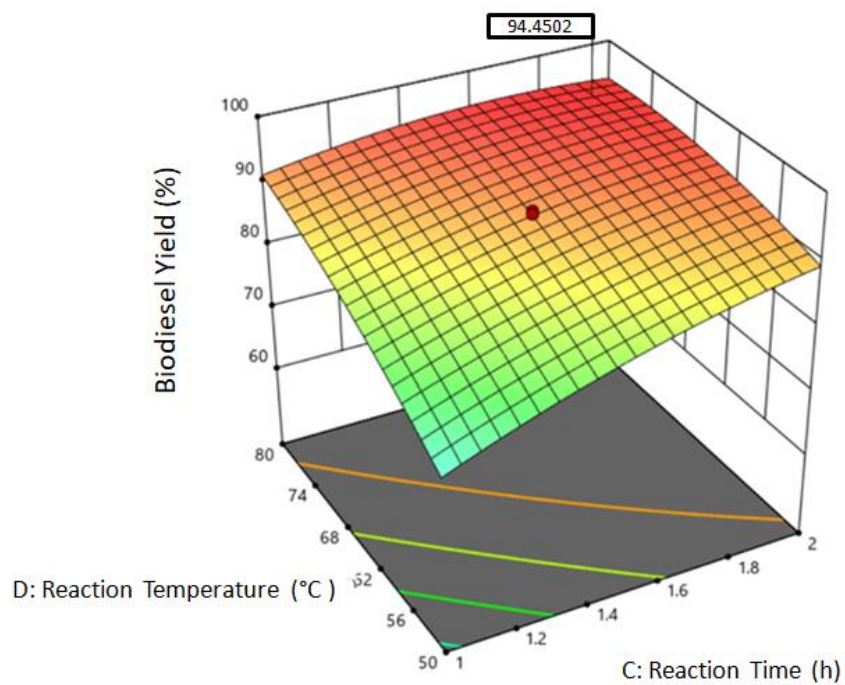
(b)

Figure 4.10: Interaction Effect between Catalyst Concentration and Reaction Temperature on Biodiesel Yield for the (a) Chicken Eggshell Model and (b) Ostrich Eggshell Model.

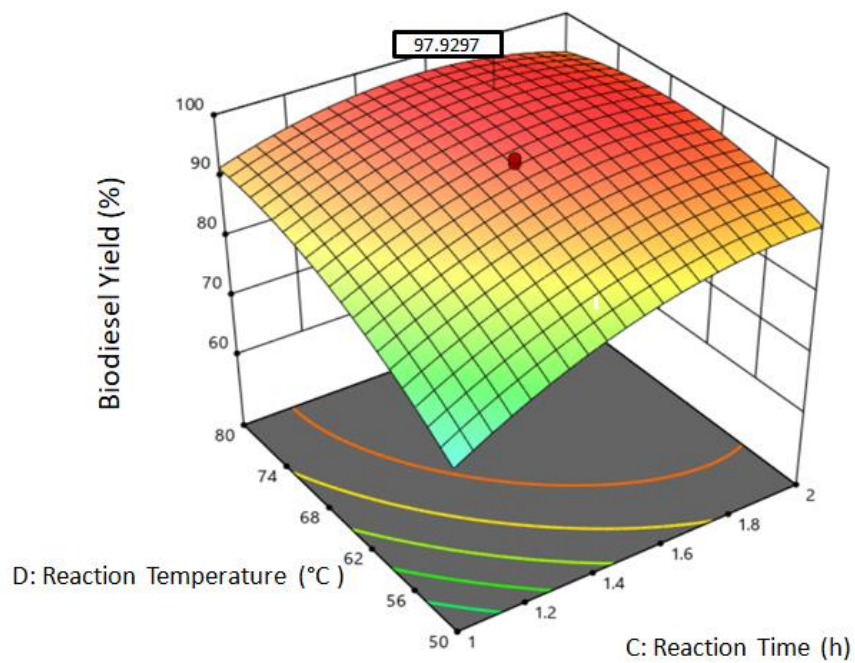
4.2.2 (f) Interaction between Reaction Time (C) and Reaction Temperature (D)

The interactive term CD was significant in both chicken eggshell model and ostrich eggshell model. This might show that the combination of reaction time and reaction temperature possessed a dominant influence on the biodiesel yield. This was because the *p*-value of the interactive term CD for both models was less than 0.0001, which was the lowest compared to the *p*-values of other interactive terms as shown in Table 4.10 and 4.11. Figure 4.11 shows the interactive effect of reaction time and reaction temperature on the biodiesel yield. For the chicken eggshell model, it was observed from Figure 4.11 (a) that increasing the reaction time from 1 hour to 1.9 hours and reaction temperature from 50 °C to around 77 °C increased the biodiesel yield to a maximum value of around 94 %. For the ostrich eggshell model as shown in Figure 4.11 (b), increasing the reaction time from 1 hour to 1.6 hours and reaction temperature from 50 °C to 74 °C increased the biodiesel yield to a maximum value of around 97 %. The biodiesel yield increased when reaction time was increased as sufficient time was needed for the reactants to complete the reaction (Rabia, et al., 2018).

However, the biodiesel yield was slightly declined by extending the reaction time beyond 1.9 hours in chicken eggshell model and beyond 1.6 hours in ostrich eggshell model. This indicated that prolonged reaction time did not enhance the biodiesel yield and it might lead to reverse reaction when the chemical equilibrium is reached, causing the yield to drop (Shuit, et al., 2012). Furthermore, raising the temperature beyond the optimum value also caused a decline in the biodiesel yield. This might probably due to the decrease in polarity and excess vaporisation of the methanol at high temperatures which lead to a drop in biodiesel yield (Abdullah, et al., 2017).



(a)



(b)

Figure 4.11: Interaction Effect between Reaction Time and Reaction Temperature on Biodiesel Yield for the (a) Chicken Eggshell Model and (b) Ostrich Eggshell Model.

4.2.3 Optimisation of Process Parameters

The optimum value of biodiesel yield for each model can be determined by carrying out the optimisation process using the Design Expert software. The desired goal for each process parameter was set within the studied range while the response (biodiesel yield) was set as maximum to obtain the best performance. The studied ranges for all the process parameters were presented in Table 4.15.

Then, the optimum operating conditions of biodiesel production for the respective models were established and were summarised in Table 4.16. For the chicken eggshell model, the maximum biodiesel yield of 95.65 % was recorded at methanol to oil ratio of 11.40:1, CaO catalyst loading of 1.43 wt. %, reaction time of 1.7 hours and reaction temperature of 79.20 °C. Next, methanol to oil ratio of 10.07:1 and CaO catalyst loading of 1.61 wt. % reacted at 75.68 °C for 1.4 hours gave an optimum biodiesel yield of 97.45 % for the ostrich eggshell model. The software also revealed that a biodiesel yield of 93.11 % could be obtained for the snail shell model with the following parameters: methanol to oil ratio of 6.84:1, CaO catalyst loading of 8.33 wt. % and reaction duration of 1.9 hours. Furthermore, methanol to oil volumetric ratio of 65.16 %, CaO catalyst loading of 7.52 wt. % and reaction duration of 125 minutes was suggested to be the optimum operating condition for the *Donax deltoideus* shell model to achieve a biodiesel yield of 96.95 %. Lastly, a biodiesel yield of 98 % was obtained with methanol to oil ratio of 8.58:1, CaO catalyst loading of 1.89 wt. % and reaction time of 113 minutes for the *Malleus malleus* shell model.

The results obtained from the software were compared with the experimental results obtained from the journals. The discrepancy was within 2 % error values, confirming that the predicted models generated by CCD were accurate and valid.

Table 4.15: Constraints Used to Optimise the Biodiesel Yield.

Parameter	Goal	Chicken Eggshell		Ostrich Eggshell		Snail Shell Model		<i>Donax deltoids</i>		<i>Malleus malleus</i>	
		Model		Model		Model		shell Model		shell Model	
		Lower Limit	Upper Limit	Lower Limit	Upper Limit	Lower Limit	Upper Limit	Lower Limit	Upper Limit	Lower Limit	Upper Limit
A: Methanol to oil ratio	In Range	8:1	12:1	8:1	12:1	6:1	9:1	62 %	82 %	6:1	12:1
B: Catalyst Concentration	In Range	1 wt. %	2 wt. %	1 wt. %	2 wt. %	6 wt. %	12 wt. %	6 wt. %	10 wt. %	1 wt. %	2 wt. %
C: Reaction Time	In Range	1 hour	2 hours	1 hour	2 hours	1 hour	3 hours	120 minutes	180 minutes	60 minutes	120 minutes
D: Reaction Temperature	In Range	50 °C	80 °C	50 °C	80 °C	-	-	-	-	-	-
Biodiesel Yield	Maximise	65.2 %	94.5 %	65.7 %	97.3 %	68 %	92.6 %	23.9 %	95.1 %	30 %	97 %

Table 4.16: Optimum Operating Conditions for Biodiesel Production for Each Model.

Model	Methanol to Oil Ratio	Catalyst Concentration	Reaction Time	Reaction Temperature	Maximum Biodiesel Yield Obtained from Software	Experimental Biodiesel Yield	Percentage Difference
Chicken Eggshell- Derived CaO Catalyst	11.40:1	1.43 wt. %	1.7 hours	79.20 °C	95.65 %	94 %	1.73 %
Ostrich Eggshell- Derived CaO Catalyst	10.07:1	1.61 wt. %	1.4 hours	75.68 °C	97.45 %	96 %	1.49 %
Snail Shell-Derived CaO Catalyst	6.84:1	8.33 wt. %	1.9 hours	-	93.11 %	92 %	1.19 %
<i>Donax deltoideus</i> Shell- Derived CaO Catalyst	65.16 %	7.52 wt. %	125 minutes	-	96.95 %	96.5 %	0.46 %
<i>Malleus malleus</i> Shell- Derived CaO Catalyst	8.58:1	1.89 wt. %	113 minutes	-	98 %	97 %	1.02 %

CHAPTER 5

CONCLUSIONS AND RECOMMENDATIONS

5.1 Conclusions

In this study, CaO catalysts that prepared from various biomass sources were reviewed through the characterisation studies. The SEM images depicted that rough and porous structures with agglomerates were developed after the calcination process, indicating the destruction of structure under high temperatures as a result of the decomposition of CaCO_3 to CaO. This finding could be affirmed by the EDX results which revealed that CaO was the major phase present in the catalyst samples after calcination. Next, the results of BET analysis showed that the surface area of the catalyst samples increased after the calcination process. This could actually enhance the activity of the catalysts.

From the TGA analysis, it was found that the catalysts experienced two stages of weight loss during the thermal treatment. The first weight loss was due to the removal of absorbed moisture and organic compounds from the samples while the second weight loss was due to the decomposition of CaCO_3 in the samples into CaO together with the release of carbon dioxide. Then, the FTIR spectrum of the calcined catalysts showed that the intensity of the peaks corresponding to the CO_3^{2-} declined or eventually disappeared which once again revealed the decomposition of CaCO_3 through calcination process. Furthermore, the XRD patterns of the catalysts showed peaks at around 32° , 37° , 54° , 64° and 67° which were attributed to the presence of CaO in the catalyst samples.

On the other hand, the influences of different process parameters on the biodiesel yield were determined by using CCD in the Design Expert software. The results showed that the biodiesel yield increased when the methanol to oil molar ratio, catalyst concentration, reaction time and reaction temperature increased to some extent. However, further increment of those parameters beyond their optimum values in the model would cause a decline in the biodiesel yield.

Based on the optimisation results obtained for different biomass-derived CaO catalyst models, the maximum biodiesel yield for the chicken eggshell model was found to be 95.65 % at 11.40:1 methanol to oil ratio, 1.43 wt. % CaO catalyst loading, 1.7 hours reaction time and reaction temperature of 79.20 °C. For the ostrich eggshell model, methanol to oil ratio of 10.07:1, CaO catalyst loading of 1.61 wt. %, reaction time of 1.4 hours and reaction temperature of 75.68 °C gave an optimum biodiesel yield of 97.45 %. Next, a maximum biodiesel yield of 93.11 % can be achieved for the snail shell model at 6.84:1 methanol to oil ratio, 8.33 wt. % CaO catalyst concentration and 1.9 hours reaction time. For the *Donax deltoids* shell model, a maximum biodiesel yield of 96.95% was found to be achieved with methanol to oil volumetric ratio of 65.16 %, CaO catalyst loading of 7.52 wt. % at 125 minutes of reaction time. Then, methanol to oil ratio of 8.58:1, CaO catalyst loading of 1.89 wt. % and reaction time of 113 minutes was suggested to be the optimum operating condition for the *Malleus malleus* shell model to achieve a biodiesel yield of 98 %.

The present study proved that a variety of waste biomass can be utilised as a source of CaCO₃ to generate CaO catalyst through the calcination process, which can then be applied in the transesterification of waste cooking oil to produce a high yield of biodiesel. The utilisation of biomass-derived CaO catalyst could be a viable choice for the sustainable production of biodiesel as it is easily available, environmentally friendly, low-cost to produce and can help to resolve the waste disposal problems.

5.2 Recommendations for Future Work

As the information required for the catalyst characterisation studies and the input data needed for the response surface modelling were retrieved from various literary journals, the comparison of the results might be affected by the inconsistent operating conditions in different journals. Hence, in order to enhance the accuracy of the result and ensure an effective result's comparison in future studies, it is recommended that the catalyst preparation conditions such as the calcination time and calcination temperature should be the same for different biomass-derived CaO catalysts.

Furthermore, the study of the effects of different process parameters on biodiesel yield and the interactions between parameters should be conducted under the same ranges of operating conditions to ease the comparison of results. In addition, further study on the regeneration and reusability of spent CaO catalysts can be conducted to investigate the feasibility of the biomass-derived CaO catalysts in practical applications.

REFERENCES

- Abdullah, S., Hanapi, N., Azid, A., Umar, R., Juahir, H., Khatoon, H. and Endut, A., 2017. A review of biomass-derived heterogeneous catalyst for a sustainable biodiesel production. *Renewable and Sustainable Energy Reviews*, 70, pp. 1040-1051.
- Agarwal, A., Bijwe, J. and Das, L., 2003. Effect of biodiesel utilization on wear of vital parts in compression ignition engine. *Journal of Engineering for Gas Turbines and Power*, 125(2), pp. 604-611.
- Agarwal, M., Chauhan, G., Chaurasia, S.P. and Singh, K., 2011. Study of catalytic behavior of KOH as homogeneous and heterogeneous catalyst for biodiesel production. *Journal of the Taiwan Institute of Chemical Engineers*, 43(1), pp. 89-94.
- Al-Muhtaseb, A.H., Jamil, F., Al-Haj, L., Myint, M.T., Mahmoud, E., Ahmad, M.N., Hasan, A.O. and Rafiq, S., 2018. Biodiesel production over a catalyst prepared from biomass-derived waste date pits. *Biotechnology Reports*, 20(2), pp. 284-296.
- Amadine, O., Essamlali, Y., Fihri, A., Larzek, M. and Zahouily, M., 2017. Effect of calcination temperature on the structure and catalytic performance of copper-ceria mixed oxide catalysts. *RSC Advances*, 7(21), pp. 12586-12597.
- Atadashi, I., Aroua, M., Abdul Aziz, A. and Sulaiman, N., 2013. The effects of catalysts in biodiesel production: a review. *Journal of Industrial and Engineering Chemistry*, 19(1), pp. 14-26.
- Awogbemi, O., Inambao, F. and Onuh, E., 2020. Modification and characterization of chicken eggshell for possible catalytic applications. *The Scientific World Journal*, 6(10), pp. 528-534.
- Babaki, M., Yousefi, M., Habibi, Z. and Mohammadi, M., 2017. Process optimization for biodiesel production from waste cooking oil using multi-enzyme systems through response surface methodology. *Renewable Energy*, 105, pp. 465-472.
- Behera, S., Meena, H., Chakraborty, S. and Meikap, B., 2018. Application of response surface methodology (RSM) for optimization of leaching parameters for ash reduction from low-grade coal. *International Journal of Mining Science and Technology*, 28(4), pp. 621-629.
- Bhattacharya, S., 2021. Central composite design for response surface methodology and its application in pharmacy. *Journal of Engineering Science*, 2 (1), pp. 477-490.

- Bharti, R., Guldhe, A., Kumar, D. and Singh, B., 2020. Solar irradiation assisted synthesis of biodiesel from waste cooking oil using calcium oxide derived from chicken eggshell. *Fuel*, 27(3), pp. 117-178.
- Borges, M.E. and Díaz, L., 2012. Recent developments on heterogeneous catalysts for biodiesel production by oil esterification and transesterification reactions: a review. *Renewable and Sustainable Energy Reviews*, 16(5), pp. 2839–2849.
- Boey, P., Maniam, G. and Hamid, S., 2011. Performance of calcium oxide as a heterogeneous catalyst in biodiesel production: a review. *Chemical Engineering Journal*, 168(1), pp. 15-22.
- Buasri, A., Worawanitchaphong, P., Trongyong, S. and Loryuenyong, V., 2014. Utilization of scallop waste shell for biodiesel production from karanja oil – optimization using taguchi method. *APCBEE Procedia*, 8, pp. 216-221.
- Chaiyut, N., Buasri, A., Loryuenyong, V., Worawanitchaphong, P. and Trongyong, S., 2013. Calcium oxide derived from waste shells of mussel, cockle, and scallop as the heterogeneous catalyst for biodiesel production. *The Scientific World Journal*, 20(3), pp. 110-117.
- Chakraborty, R., Chatterjee, S., Mukhopadhyay, P. and Barman, S., 2016. Progresses in waste biomass derived catalyst for production of biodiesel and bioethanol: a review. *Procedia Environmental Sciences*, 35, pp. 546-554.
- Chen, G., Shan, R., Shi, J. and Yan, B., 2014. Ultrasonic-assisted production of biodiesel from transesterification of palm oil over ostrich eggshell-derived CaO catalysts. *Bioresource Technology*, 171, pp. 428-432.
- Chumuang, N. and Punsuvon, V., 2017. Response surface methodology for biodiesel production using calcium methoxide catalyst assisted with tetrahydrofuran as cosolvent. *Journal of Chemistry*, 2017, pp. 111-119.
- Colombo, K., Ender, L. and Barros, A., 2017. The study of biodiesel production using CaO as a heterogeneous catalytic reaction. *Egyptian Journal of Petroleum*, 26(2), pp. 341-349.
- Correia, L., Saboya, R., Sousa Campelo, N., Cecilia, J., Rodríguez-Castellón, E., Cavalcante, C. and Vieira, R., 2014. Characterization of calcium oxide catalysts from natural sources and their application in the transesterification of sunflower oil. *Bioresource Technology*, 151, pp. 207-213.
- Dawodu, F., Ayodele, O., Xin, J., Zhang, S. and Yan, D., 2014. Effective conversion of non-edible oil with high free fatty acid into biodiesel by sulphonated carbon catalyst. *Applied Energy*, 114, pp. 819-826.
- Deng, J., Li, M. and Wang, Y., 2016. Biomass-derived carbon: synthesis and applications in energy storage and conversion. *ChemInform*, 47(46), pp. 114-121.

- De, S., Balu, A.M., Van der Waal, J.C. and Luque, R., 2015. Biomass-derived porous carbon materials: synthesis and catalytic applications. *ChemCatChem*, 7, pp. 1608 – 1629.
- Degfie, T.A., Mamo, T.T. and Mekonnen, Y.S., 2019. Optimized biodiesel production from waste cooking oil using calcium oxide nano-catalyst. *Scientific Reports*, 9(1), pp. 182-189.
- Deshpande, S., Sunol, A. and Philippidis, G., 2017. Status and prospects of supercritical alcohol transesterification for biodiesel production. *Wiley Interdisciplinary Reviews: Energy and Environment*, 6(5), pp. 252-259.
- Dhmees, A.S., Rashad, A.M. and Abdullah, E.S., 2019. Calcined petroleum scale-CaO a cost effective catalyst for used cooking oil methanolysis. *Egyptian Journal of Chemistry*, 63(3), pp. 1033-1044.
- Diamantopoulos, N., 2015. Comprehensive review on the biodiesel production using solid acid heterogeneous catalysts. *Journal of Thermodynamics & Catalysis*, 06(01), pp. 378-385.
- Domingues, C., Correia, M., Carvalho, R., Henriques, C., Bordado, J. and Dias, A., 2012. Vanadium phosphate catalysts for biodiesel production from acid industrial by-products. *Journal of Biotechnology*, 164(3), pp. 433-440.
- El-Gendy, N.S., Abu, A.S. and Aziz, H.A., 2014. The optimization of biodiesel production from waste frying sunflower oil using a heterogeneous catalyst. *Energy Sources, Part A: Recovery, Utilization, and Environmental Effects*, 36(15), pp. 1615-1625.
- Erhan, S. and Singh, N.P., 2007. Formation of CaO from thermal decomposition of calcium carbonate in the presence of carboxylic acids. *Journal of Thermal Analysis and Calorimetry*, 89(1), pp. 159-162.
- Engin, B., Demirtas, H. and Eken, M., 2006. Temperature effects on egg shells investigated by XRD, IR and ESR techniques. *Radiation Physics and Chemistry*, 75(2), pp. 268-277.
- Fayyazi, E., Ghobadian, B., Bovenkamp, H., Najafi, G., Hosseinzadehsamani, B., Heeres, H. and Yue, J., 2018. Optimization of biodiesel production over chicken eggshell-derived CaO catalyst in a continuous centrifugal contactor separator. *Industrial & Engineering Chemistry Research*, 57(38), pp. 12742-12755.
- Ferronato, N. and Torretta, V., 2019. Waste mismanagement in developing countries: a review of global issues. *International Journal of Environmental Research and Public Health*, 16(6), pp. 1060-1066.

- Ferreira, S., Bruns, R., Ferreira, H., Matos, G., David, J., Brandão, G., da Silva, E., Portugal, L., dos Reis, P., Souza, A. and dos Santos, W., 2007. Box-behken design: an alternative for the optimization of analytical methods. *Analytica Chimica Acta*, 597(2), pp. 179-186.
- Flores, K., Omega, J., Cabatingan, L., Go, A.W., Agapay, R. and Ju, Y.H., 2019. Simultaneously carbonized and sulfonated sugarcane bagasse as solid acid catalyst for the esterification of oleic acid with methanol. *Renewable Energy*, 130, pp. 510-523.
- Geng, L., Yu, G., Wang, Y. and Zhu, Y.X., 2012. Ph-SO₃H-modified mesoporous carbon as an efficient catalyst for the esterification of oleic acid. *Applied Catalyst A: General*, 427-428, pp. 137-144.
- Gendy, N., Deriase, S. and Hamdy, A., 2014. The optimization of biodiesel production from waste frying corn oil using snails shells as a catalyst. *Energy Sources, Part A: Recovery, Utilization, and Environmental Effects*, 36(6), pp. 623-637.
- Guan, G., Kusakabe, K. and Yamasaki, S., 2009. Tri-potassium phosphate as a solid catalyst for biodiesel production from waste cooking oil. *Fuel Processing Technology*, pp. 211-218.
- Guldhe, A., Singh, P., Ansari, F., Singh, B. and Bux, F., 2017. Biodiesel synthesis from microalgal lipids using tungstated zirconia as a heterogeneous acid catalyst and its comparison with homogeneous acid and enzyme catalysts. *Fuel*, 187(1), pp. 180-188.
- Gupta, A. and Rathod, V., 2019. Solar radiation as a renewable energy source for the biodiesel production by esterification of palm fatty acid distillate. *Energy*, 182, pp. 795-801.
- Gui, M.M., Lee, K.T. and Bhatia, S., 2008. Feasibility of edible oil vs. non-edible oil vs. waste edible oil as biodiesel feedstock. *Energy*, 33(11), pp. 1646-1653.
- Kar, R., Gupta, O. and Das, K., 2012. Biodiesel production and process optimization. *International Journal of Scientific and Research Publications*, 2(6), pp. 112-118.
- Karimifard, S. and Alavi, M., 2018. Application of response surface methodology in physicochemical removal of dyes from wastewater: a critical review. *Science of The Total Environment*, 640-641, pp. 772-797.
- Khan, S., Siddique, R., Sajjad, W., Nabi, G., Hayat, K., Duan, P. and Yao, L., 2017. Biodiesel production from algae to overcome the energy crisis. *HAYATI Journal of Biosciences*, 24(4), pp. 163-167.

- Kouzu, M., Kasuno, T., Tajika, M., Sugimoto, Y., Yamanaka, S., Hidaka, J., 2007. Calcium oxide as a solid base catalyst for transesterification of soybean oil and its application to biodiesel production. *Fuel*, 87(12), pp. 2798–2806.
- Lam, M.K., Lee, K.T. and Mohamed, A.R., 2010. Homogeneous, heterogeneous and enzymatic catalysis for transesterification of high free fatty acid oil (waste cooking oil) to biodiesel: a review. *Biotechnology Advances*, 28(4), pp. 500-518.
- Laskar, I.B., Rajkumari, K., Gupta, R., Chatterjee, S., Paul, B. and Rokhum, L., 2018. Waste snail shell derived heterogeneous catalyst for biodiesel production by the transesterification of soybean oil. *RSC Advances*, 8(36), pp. 20131-20142.
- Leung, D., Wu, X. and Leung, M., 2010. A review on biodiesel production using catalyzed transesterification. *Applied Energy*, 87(4), pp. 1083-1095.
- Liu, X., He, H., Wang, Y., Zhu, S. and Piao, X., 2008. Transesterification of soybean oil to biodiesel using CaO as a solid base catalyst. *Fuel*, 87(2), pp. 216–221.
- Liu, T., Li, Z., Li, W., Shi, C. and Wang, Y., 2013. Preparation and characterization of biomass carbon-based solid acid catalyst for the esterification of oleic acid with methanol. *Bioresource Technology*, 133, pp. 618-621.
- Liu, X.Y., Huang, M., Ma, H.L., Zhang, Z.Q., Gao, J.M., Zhu, Y.L, Han, X.J. and Guo, X.Y., 2010. Preparation of a carbon-based solid acid catalyst by sulfonating activated carbon in a chemical reduction process. *Molecules*, 15(10), pp. 7188-7196.
- Lorza, R.L., Calvo, M.Á.M., Labari, C.B. and Fuente, P.J.R., 2018. Using the multi-response method with desirability functions to optimize the zinc electroplating of steel screws. *Metals*, 8(9), pp.1–20.
- Maceiras, R., Vega, M., Costa, C., Ramos, P. and Marquez, M.C., 2009. Effect of methanol content on enzymatic production of biodiesel from waste frying oil. *Fuel*, 88, pp. 2130-2134.
- Margaretha, Y., Prastyo, H., Ayucitra, A. and Ismadji, S., 2012. Calcium oxide from *Pomacea* sp. shell as a catalyst for biodiesel production. *International Journal of Energy and Environmental Engineering*, 3(1), pp. 133-140.
- Maneerung, T., Kawi, S. and Wang, C., 2015. Biomass gasification bottom ash as a source of CaO catalyst for biodiesel production via transesterification of palm oil. *Energy Conversion and Management*, 92, pp. 234-243.
- Meher, L., Vidyasagar, D. and Naik, S., 2016. Technical aspects of biodiesel production by transesterification: a review. *Renewable and Sustainable Energy Reviews*, 10(3), pp. 248-268.

- Mishra, B., 2012. Eco-friendly biodiesel as an alternative fuel for diesel-engine. *IOSR Journal of Applied Chemistry*, 2(4), pp. 41-45.
- Mohamed, M., Rashidi, N., Yusup, S., Teong, L., Rashid, U. and Ali, R., 2012. Effects of experimental variables on conversion of cockle shell to calcium oxide using thermal gravimetric analysis. *Journal of Cleaner Production*, 37, pp. 394-397.
- Narowska, B., Kulazynski, M. and Lukaszewicz, M., 2020. Application of activated carbon to obtain biodiesel from vegetable oils. *Catalysts*, 10(9), pp. 1049-1063.
- Niju, S., Vishnupriya, G. and Balajii, M., 2019. Process optimization of Calophyllum inophyllum-waste cooking oil mixture for biodiesel production using *Donax deltoides* shells as heterogeneous catalyst. *Sustainable Environment Research*, 29, pp. 113-123.
- Oliveira, C., Teleken, H.J. and Alves, H., 2020. Catalytic efficiency of the eggshell calcined and enriched with glycerin in the synthesis of biodiesel from frying residual oil. *Environmental Science and Pollution Research*, 27(15), pp. 17878-17890.
- Omole, J. and Dauda, B., 2016. Fourier transform infrared spectroscopy (FTIR) and scanning electron microscopy (SEM) analysis of chemically treated bagasse fibre. *American Chemical Science Journal*, 15(2), pp. 111-119.
- Ochkin, A., Gladilov, D. and Nekhaevskiy, S., 2012. Optimization of solvent extraction reprocessing using mathematical modelling. *Procedia Chemistry*, 7, pp. 315-321.
- Panpraneecharoen, S., Punsuvon, V. and Pueemchalad, C., 2015. Comparison of homogeneous and heterogeneous catalysts in biodiesel production from pongamia pinnata oil. *Asian Journal of Chemistry*, 27(3), pp. 1023-1027.
- Piker, A., Tabah, B., Perkas, N. and Gedanken, A., 2016. A green and low-cost room temperature biodiesel production method from waste oil using egg shells as catalyst. *Fuel*, 182, pp. 34-41.
- Quintella, C., Santos, W., Ferreira, S., Neto, B. and Bosque-Sendra, J., 2004. Doehlert matrix: a chemometric tool for analytical chemistry—review. *Talanta*, 63(4), pp. 1061-1067.
- Rashid, U., Anwar, F., Ashraf, M., Saleem, M. and Yusup, S., 2011. Application of response surface methodology for optimizing transesterification of *Moringa oleifera* oil: biodiesel production. *Energy Conversion and Management*, 52(8), pp. 3034-3042.

Rabia, R., Niju, S., Sumithra Devi, K., Naveen Kumar, M. and Balajii, M., 2018. Modified malleus malleus shells for biodiesel production from waste cooking oil: an optimization study using box-behnken design. *Waste and Biomass Valorization*, 11(3), pp. 793-806.

Ramli, A. and Farooq, M., 2015. Optimization of process parameters for the production of biodiesel from waste cooking oil in the presence of bifunctional γ -Al₂O₃-CeO₂ supported catalysts. *Malaysian Journal of Analytical Sciences*, 19(1), pp. 8-19.

Reddy, A., Saleh, A., Islam, M. and Hamdan, S., 2017. Active razor shell CaO catalyst synthesis for jatropha methyl ester production via optimized two-step transesterification. *Journal of Chemistry*, 2(1), pp. 180-200.

Roschat, W., Siritanon, T., Kaewpuang, T., Yoosuk, B. and Promarak, V., 2016. Economical and green biodiesel production process using river snail shells-derived heterogeneous catalyst and co-solvent method. *Bioresource Technology*, 209, pp. 343-350.

Sakkas, V., Islam, M., Stalikas, C. and Albanis, T., 2010. Photocatalytic degradation using design of experiments: a review and example of the Congo red degradation. *Journal of Hazardous Materials*, 175(1-3), pp. 33-44.

Santya, G., Maheswaran, T. and Yee, K., 2019. Optimization of biodiesel production from high free fatty acid river catfish oil (*pangasius hypothalamus*) and waste cooking oil catalyzed by waste chicken egg shells derived catalyst. *SN Applied Sciences*, 1(2), pp. 211-220.

Saffari, M., 2018. Response surface methodological approach for optimizing the removal of cadmium from aqueous solutions using pistachio residues biochar supported/non-supported by nanoscale zero-valent iron. *Main Group Metal Chemistry*, 41(5-6), pp. 167-181.

Salamatinia, B., Mootabadi, H., Bhatia, S. and Abdullah, A., 2010. Optimization of ultrasonic-assisted heterogeneous biodiesel production from palm oil: a response surface methodology approach. *Fuel Processing Technology*, 91(5), pp. 441-448.

Sarno, M. and Iuliano, M., 2019. Biodiesel production from waste cooking oil. *Green Processing and Synthesis*, 8(1), pp. 828-836.

Silva, G., Camargo, F. and Ferreira, A., 2011. Application of response surface methodology for optimization of biodiesel production by transesterification of soybean oil with ethanol. *Fuel Processing Technology*, 92(3), pp. 407-413.

Sharma, Y., Singh, B. and Korstad, J., 2011. Latest developments on application of heterogeneous basic catalysts for an efficient and eco friendly synthesis of biodiesel: a review. *Fuel*, 90(4), pp. 1309-1324.

- Shohaimi, N. A. and Marodzi, F. N. S., 2018. Transesterification of waste cooking oil in biodiesel production utilizing CaO/Al₂O₃ heterogeneous catalyst. *Malaysian Journal of Analytical Sciences*, 22(1), pp. 157–165.
- Shuit, S.H., Ong, Y.T., Lee, K.T., Subhash, B. and Tan, S.H., 2012. Membrane technology as a promising alternative in biodiesel production: a review. *Biotechnology Advances*, 30(6), pp. 1364-1380.
- Shin, H., An, S., Sheikh, R., Park, Y. and Bae, S., 2012. Transesterification of used vegetable oils with a Cs-doped heteropolyacid catalyst in supercritical methanol. *Fuel*, 96, pp. 572-578.
- Smith, S., Oopathum, C., Weeramongkhonlert, V., Smith, C., Chaveanghong, S., Ketwong, P. and Boonyuen, S., 2013. Transesterification of soybean oil using bovine bone waste as new catalyst. *Bioresource Technology*, 143, pp. 686-690.
- Sun, Y., Sage, V. and Sun, Z., 2017. An enhanced process of using direct fluidized bed calcination of shrimp shell for biodiesel catalyst preparation. *Chemical Engineering Research and Design*, 126, pp. 142-152.
- Takeuchi, K., Shiroyama, H., Saitō, O. and Matsuura, M., 2018. The effect of biodiesel production on greenhouse gas emission reductions. *Biodiesels and Sustainability*, 22, pp. 530-711.
- Tremblay, A.Y., Cao, P. and Dubé, M., 2008. Biodiesel production using ultralow catalyst concentrations. *Energy & Fuels*, 22(4), pp. 2748-2755.
- Tan, Y.H., Abdullah, M., Nolasco, C. and Yap, T.Y., 2015. Waste ostrich- and chicken-eggshells as heterogeneous base catalyst for biodiesel production from used cooking oil: catalyst characterization and biodiesel yield performance. *Applied Energy*, 160, pp. 58-70.
- Tan, Y.H., Abdullah, M., Nolasco, C. and Ahmad, N., 2017. Application of RSM and taguchi methods for optimizing the transesterification of waste cooking oil catalyzed by solid ostrich and chicken-eggshell derived CaO. *Renewable Energy*, 114, pp. 437-447.
- Titirici, M., Thomas, A., Yu, S., Müller, J. and Antonietti, M., 2007. A direct synthesis of mesoporous carbons with bicontinuous pore morphology from crude plant material by hydrothermal carbonization. *Chemistry of Materials*, 19(17), pp. 4205-4212.
- Vadery, V., Narayanan, B., Ramakrishnan, R., Cherikkallinmel, S., Sugunan, S., Narayanan, D. and Sasidharan, S., 2014. Room temperature production of jatropha biodiesel over coconut husk ash. *Energy*, 70, pp. 588-594.
- Villa, A., Tessonier, J.P., Majoulet, O., Su, D. and Schlögl, R., 2010. Transesterification of triglycerides using nitrogen-functionalized carbon nanotubes. *ChemSusChem*, 3(2), pp. 241-245.

- Viriya-empikul, N., Krasae, P., Puttasawat, B., Yoosuk, B., Chollacoop, N. and Faungnawakij, K., 2010. Waste shells of mollusk and egg as biodiesel production catalysts. *Bioresource Technology*, 101(10), pp. 3765-3767.
- Verma, P., Stevanovic, S., Zare, A., Dwivedi, G., Chu Van, T., Davidson, M., Rainey, T., Brown, R. and Ristovski, Z., 2019. An overview of the influence of biodiesel, alcohols, and various oxygenated additives on the particulate matter emissions from diesel engines. *Energies*, 12(10), pp. 192-198.
- Wang, S., Yan, W. and Zhao, F., 2019. Recovery of solid waste as functional heterogeneous catalysts for organic pollutant removal and biodiesel production. *Chemical Engineering Journal*, 40(1), pp. 104-126.
- Wei, Z., Xiong, D., Duan, P., Ding, S., Li, Y., Li, L., Niu, P. and Chen, X., 2019. Preparation of carbon-based solid acid catalysts using rice straw biomass and their application in hydration of α -Pinene. *Catalysts*, 10(2), pp. 213-221.
- Wong, W.Y., Lim, S., Pang, Y.L., Shuit, S.H., Chen, W.H. and Lee, K.T., 2020. Synthesis of renewable heterogeneous acid catalyst from oil palm empty fruit bunch for glycerol-free biodiesel production. *Science of The Total Environment*, 727, pp. 138-144.
- Yin, X., Duan, X., You, Q., Dai, C., Tan, Z. and Zhu, X., 2016. Biodiesel production from soybean oil deodorizer distillate using calcined duck eggshell as catalyst. *Energy Conversion and Management*, 112, pp. 199-207.
- Yuan, X., Liu, J., Zeng, G., Shi, J., Tong, J. and Huang, G., 2008. Optimization of conversion of waste rapeseed oil with high FFA to biodiesel using response surface methodology. *Renewable Energy*, 33(7), pp. 1678-1684.
- Zhang, M., Sun, A., Meng, Y., Wang, L., Jiang, H. and Li, G., 2014. Catalytic performance of biomass carbon-based solid acid catalyst for esterification of free fatty acids in waste cooking oil. *Catalysis Surveys from Asia*, 19(2), pp. 61-67.
- Zuleta, E., Baena, L., Rios, L. and Calderón, J., 2012. The oxidative stability of biodiesel and its impact on the deterioration of metallic and polymeric materials: a review. *Journal of the Brazilian Chemical Society*, 23(12), pp. 2159-2175.